NASW-4435

IN-18-CR
73-75
P. 84

SEMM 1

VPI/NASA Senior Design Project 1990-91

SOLAR-ELECTRIC-PROPULSION CARGO VEHICLES FOR SPLIT/SPRINT MARS MISSION

Advisors:

Professor Anthony Jakubowski
Aerospace Engineering Department
Virginia Polyechnic Institute

Davy A. Haynes
Space Exploration Initiative Office
NASA Langley Research Center

Student Members:

Christopher E. Callaghan

Michael D. Crowe

Matthew J. Swis

Marcus R. Mickney

C. Keith Montgomery

Robert Walters

Scott Thoden

June 1991

Department of Aerospace and Ocean Engineering

Virginia Polytechnic Institute and State University

Blacksburg, Virginia 24061

(NASA-CR-189983) SOLAR-ELECTRIC-PROPULSION CARGO VEHICLES FOR SPLIT/SPRINT MARS MISSION (Virginia Polytechnic Inst. and State Univ.) 84 p
CSCL 22B

N92-23526

Unclas
G3/18 0073895

Table of Contents

LIST OF FIGURES

LIST OF TABLES

ABSTRACT

In support of the proposed exploration of Mars, an unmanned cargo ferry SEMM1 (Solar Electric Mars Mission) has been designed. The vehicle is based on solar electric propulsion, and required to transport a cargo of 61,000 kilograms. The trajectory is a combination of spirals; first, out from LEO, then around the sun, then spiral down to low Mars orbit. The spacecraft produces 3.03 MWe power using photovoltaic flexible blanket arrays. Ion thrusters using argon as a propellant have been selected to drive the ship, providing about 60 Newtons of thrust in low Earth orbit. The configuration is based on two long truss beams to which the 24 individual, self-deployable, solar arrays are attached. The main body module supports the two beams and houses the computers, electrical, and control equipment. The thruster module is attached to the rear of the main body, and the cargo to the front.

1. INTRODUCTION

1.1 SEMM1 Team

Team Leader	-	Christopher Callaghan
Trajectory	-	Marcus Mickney Keith Montgomery
Propulsions	-	Michael Crowe Matthew Swis
Power System	-	Scott Thoden Robert Walters
Structures	-	Robert Walters Christopher Callaghan Matthew Swis
Communications	-	Marcus Mickney

1.2 Background

1.2a Historical Background

In May of 1990, President Bush visited Marshall Space Flight Center in Houston, Texas and made a historical speech. His words there crystallized the goals of many Americans: to land again on the Moon and establish a permanent presence there, then to send a manned mission to Mars. The President also set a date of 2019 for this momentous first landing on Mars, and NASA engineers and science fans nationwide raced back to their drawing boards. A Mars mission had long been dreamed about, but never studied in depth. A call was put out for papers and ideas that might aid in the accomplishment of the long awaited journey.

Every senior engineering class at Virginia Tech participates in a design project in their major field of study. This year one of the topics available to the Aerospace and Ocean Engineering class was the development of a conceptual design for a spacecraft that would operate in support of the Mars mission. Specifically, the design would be for an unmanned cargo ferry that could bring equipment and supplies to Mars.

1.2b Definition of Concept

The concept for a Mars cargo ferry stems from the idea of a progressive presence in deep space in support of human exploration. This idea includes the short term use of present technology to begin exploration and mapping of the Martian surface. Much work must be done before any men ever step onto the surface of another planet, including terrain mapping, atmospheric and soil sampling, and the establishment of a communication system on and around Mars.

Once newer technology has reached maturity, it would be used immediately to push the exploration ahead. Automated workers would assemble scientific bases and habitats for the humans soon to come. Orbiting satellites would be placed around the planet to provide constant communication and commands to the machines and probes on Mars. The cargo ferry will be used to bring these materials to Mars. It is required to drop the cargo module off in orbit around Mars, to be transferred down to the surface by an orbital transfer vehicle, either manned or automated. The cargo ferry is a vital workhorse in this overall plan.

1.3 Design Considerations

A design of a major space vehicle must always identify several key criteria dependent on the mission. The cargo ferry will be built with these factors in mind: mission accomplishment, proven technology, and reusability.

The main mission of the ferry is to deliver a cargo to Mars orbit. Although there will be no humans on board the ship, its cargo will be million dollar machinery, probes, and equipment. The loss of this cargo will not be easily replaceable, since most of it will be uniquely designed for this mission. The inability to perform the mission will push the calendar for Mars expansion back several years. Therefore, the craft must survive and reach its destination, and all design characteristics reflect this consideration.

To make the mission more realizable, the SEMM1 technology level will include mostly current production hardware. A cargo vessel is not a testing bed for exciting, innovative gadgetry. However, space technology is evolving at a rapid rate, and technological advances and trends should not be overlooked. Everything used on the ferry has been studied for several years by top NASA and industry engineers. By the time the ship is launched, most of the components will have been flown in space and probably improved over what is presented in this report. Performance in certain areas was projected based on what researchers predicted would be available.

The third consideration was endurance. The ship must be dependable and reusable, or the cost of its operation would overshadow its usefulness as a means of transporting cargo. Degradation was analyzed, and modularity of the components was emphasized so that easy maintenance could be performed by robots or astronauts in Earth's orbit.

1.4 Mission Scenario - General Assumptions

The construction of a cargo ferry has its place in a long list of space-related events. First and foremost is the development of a heavy lift launch vehicle (HLV) to boost the pieces of SEMM1 into Low Earth Orbit (LEO). The space shuttle is a remarkable machine and is capable of great scientific experiments, but it is not big enough or strong enough to be used for launching the cargo. A more powerful, unmanned version of the shuttle, called Shuttle-C, has been proposed and would fit the requirements for a launch vehicle. "Big, dumb boosters" are also a candidate for a comeback, having been phased out in the 1970's with the last of the Atlas launches.

The second most important milestone is the construction and operation of a large, manned, orbiting station. This station could be used for science and astronomical study, but is most important to this mission as a construction site. Current proposals for Space Station Freedom do not include such capabilities in Phase I, to be completed in 1995. Phase II, however, will include the addition of special construction bays where lunar and interplanetary vehicles may be assembled and launched. Space construction offers the opportunity for huge structures to be built that would not have been able to withstand the force of launching.

Other assumptions include the expansion of a Deep Space Network (DSN) for interplanetary communications. This will require the placement of relay satellites in Mars orbit before the cargo mission takes place. Also assumed is that Congress and the American people will continue to support progress in space, for without proper funding, the technology referenced in this paper may not exist.

1.5 Vehicle Configuration

1.5a Design Requirements

The initial requirements for SEMM1 were laid down before any research began. The cargo ferry will be capable of carrying a 61,000 kg module. This cargo will be sized according to the Shuttle-C cargo bay.

SEMM1 will be solar powered. The power collected will be used to power ion thrusters using argon as a propellant. The nature of electric propulsion makes the craft incapable of great accelerations and therefore very slow, which makes sense considering the purpose of the vehicle. The total trip time to Mars and back was suggested at around three years, since the cargo does not have to be on Mars immediately, but timely enough to keep up the pace of the exploration.

1.5b Design Evolution

The layout of the vehicle was the first step to be considered. Pictures of Solar Electric Propulsion (SEP) vehicle designs taken from other sources showed a variety of configurations. Common sense dictated that most of the system's hardware components (i.e. cargo, computers, power conversion system, communications and navigational gear) should be housed together in a module or two. Most of the configuration choices differed only in shape of the solar arrays and location of the engines.

The first concept that was considered was building the solar array as one immense flat sheet. The core module containing the cargo and ship hardware would be suspended in the center, with the ion thrusters mounted on wingtips that extended out from each corner. This design gave the thrusters clearance from the arrays and a very large moment arm that would help with maneuvers. However, it required pumping fuel from the central tanks to each wing pod, a massive support structure for the solar panels, and considerable construction and assembly in space.

Current satellites, including the Hubble Space Telescope, use a two-wing approach. The main body supports two wings of solar panels opposite each other. This gives the arrays the ability to rotate independently of the ship, and the ion thrusters could be mounted together in a single module directly behind the core body. This design was chosen early on as the most likely candidate for configuration.

Solar arrays can use various collection strategies to gather sunlight that falls on them. Research quickly showed that optical concentrators would be ideal; lightweight, efficient, and operating at a high temperature. However, difficulties with assembly of a support structure and very strict pointing tolerances eliminated the concentrators as an option and preassembled, self-deployable flat panel arrays were chosen due to their maturity, relative ease of control and less stringent rigidity requirements. In particular, the ability to be deployed automatically was a benefit when considering assembly times and complexity.

The configuration of SEMM1 uses a square-bay truss beam to anchor 24 self-deployable flexible blanket solar arrays. These arrays provide a total area of 10,057 square meters and produce 3.03 Mwe of power at average output. A multi-bandgap cell using Indium Phosphide (InP) was chosen because of the strong radiation resistance it provided. In fact, the cell suffers almost no degradation when kept above 100°C and is the key to the power system's reusability.

The above power is required to fire the ion thrusters located in the module on the rear of the central body core. The size of the thrusters was determined using an approximate optimization that balanced specific impulse, thrust, efficiency, and power consumption. The optimal thrusters were found to be about 2 meters in diameter, each capable of producing approximately 6 Newtons of thrust. The thruster module contains 13 thrusters which can be fired in various combinations to provide the thrust needed for the ship to complete various changes in orbit. The optimal specific impulse was found to be 8,000 seconds.

Xenon has also been analyzed as a possible fuel for SEMM1. Although much more expensive and volatile, xenon is denser than argon, so that the total fuel volume required for the trip was almost three times smaller. Xenon operates more efficiently, and was found to perform best when used with 1 meter diameter thrusters capable of producing 3.2 N of thrust. The specific impulse in this case is still 8,000 seconds and 29 thrusters are required to provide the same mission flexibility and redundancy.

The total mass of the cargo ferry is estimated at 120,000 kg. Using trajectory programs developed by the design team, a course for SEMM1 was charted that would spiral the ship slowly out of Earth's gravitational field. The optimal thrust was established at about 60 N at Earth. SEP is an economical way to go, but is very slow, requiring several months just to escape the influence of Earth. The ship then spirals around the sun and intercepts Mars. Once caught by the planet's gravity, the cargo vessel then spirals down to Low Mars Orbit (LMO) where it completes its mission.

The total trip time to Mars was found to be nearly two years. Cargo dropped off at Mars and fuel used on the outbound trip will reduce the total vehicle mass so that the return trip will only take one and one half years. Once in LEO, SEMM1 will rendezvous with Space Station Freedom where it will be checked, refurbished, and refueled for another trip.

1.5c Design Summary

The driving parameters in the design of SEMM1 are nearly all dependent on each other. Solutions to the mission requirements could be found only by using an iterative process of optimization that suggested a balance between weight, power, and length of mission. The main design conclusions are summarized below.

Cargo Mass	61,000 kg
Cargo Volume	30 m long by 7 m dia.
Array Area	10,368 m^2
Array Power	3.06 Mwe
Isp (Argon)	8,000 seconds
Thruster Size	2 m dia.
Thrust (LEO)	60 N
Trip to Mars	654 days
Return Trip	497 days
Initial Mass	about 120,000 kg

TABLE 1-1 SEMM1 Design Summary

2. TRAJECTORY ANALYSIS

2.1 MISSION REQUIREMENTS

Our mission is to transport 61,000 kg of cargo from low Earth orbit at an altitude of 400 km to low Mars orbit with an altitude of 500 km and inclination of 70 degrees. The ship is to be powered using solar energy and propelled by an electric propulsion system. The craft is to make this journey three times, with repairs and refueling done at an Earth-orbiting space station. For the trajectory analysis it was convenient to divide the mission into seven phases:

1) Escape from LEO/Plane change
2) Heliocentric transfer to Mars
3) Mars capture spiral
4) Mars loiter/Cargo drop
5) Mars escape spiral
6) Heliocentric transfer to Earth
7) Dock with space station at Earth

Spiral transfers were employed because of the low thrust capability of electrical thrusters. Since the cargo ferry is power limited, time was a crucial factor in our analysis.

2.2 TRAJECTORY CALCULATIONS

Initial calculations were performed using a program TRAJ which generated rough estimates of trip times and fuel required. Later, the program QUICKTOP was made available, and all orbital calculations were revised.

To begin the optimization process, a goal of a maximum round trip mission time of about three years was established. This decision was made as a compromise between shorter times (2-2.5 years) requiring higher fuel and power usage and very long transfer times.

For a moderate range of specific impulse, and an initial mass of 140,000 kg, a round-trip time of 3 yrs corresponded to an Earth-Mars transfer time of about 1.8 years. Using this time, and the values of initial estimates of vehicle mass and Isp, power was first optimized using QUICKTOP's power optimization function. Figure 2-1 shows an "optimum" power of 3.04 MW for an Isp of 8000 sec.

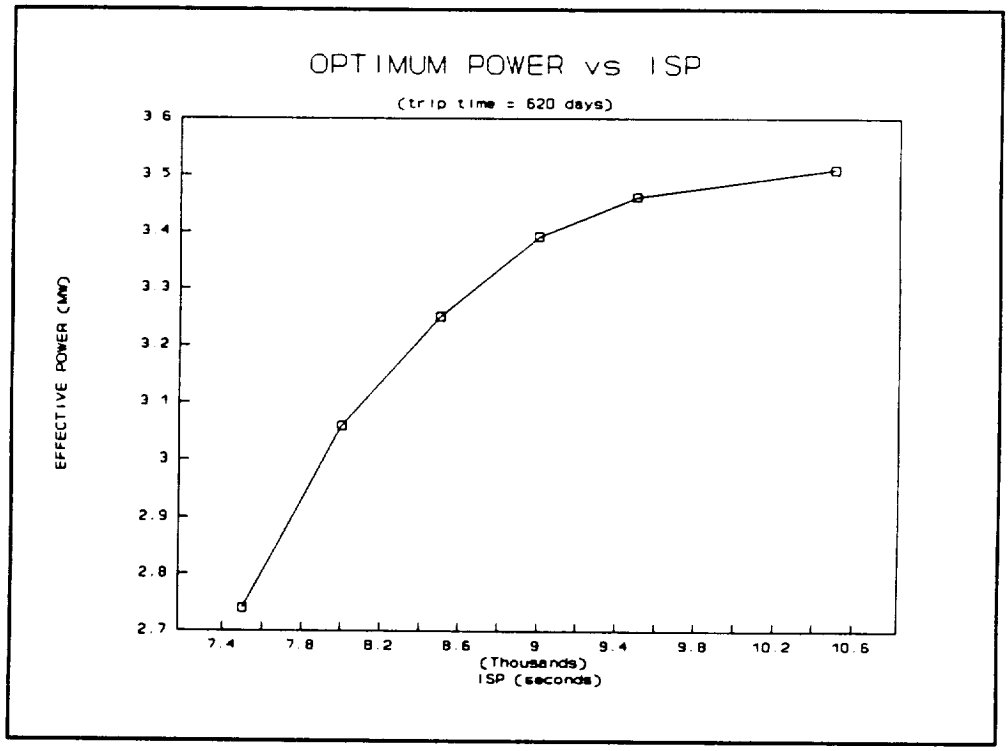

FIGURE 2-1

When this value for "optimum" power was returned to QUICKTOP, the trip time was verified (Figure 2-2). The next phase of optimization involved minimizing the fuel required (Figure 2-3) for the Earth-Mars trajectory.

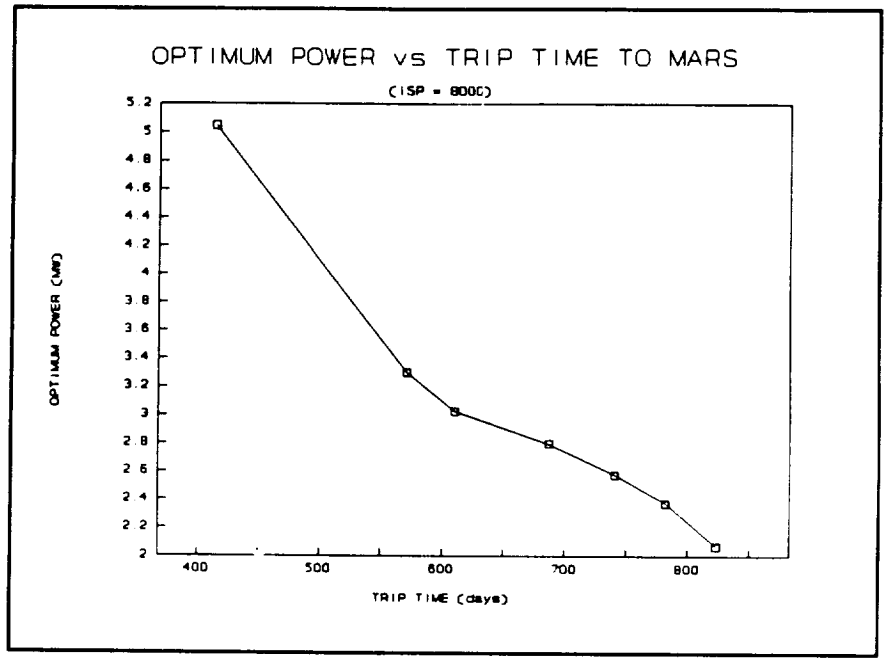

FIGURE 2-2

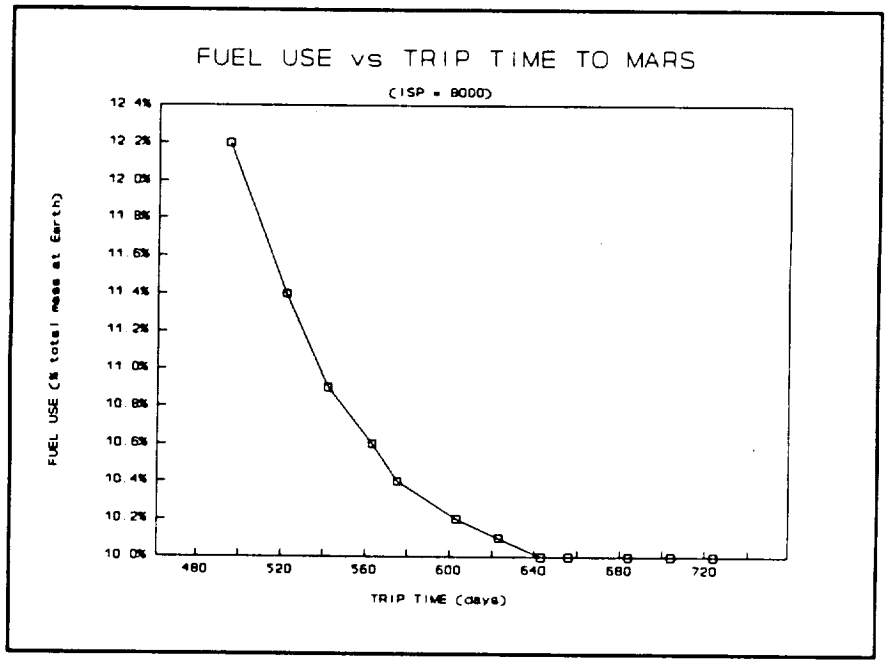

FIGURE 2-3

Since an actual minimum is not present on the plot of fuel vs trip time, an approach considering diminishing returns was used for the return voyage. As figure 2-3 indicates, after a rapid drop in fuel required with increasing trip time, the fuel consumption with time starts to level off around 630 days. These plots were generated using an effective power of 3MW (at Earth), and an Isp of 8000 sec.

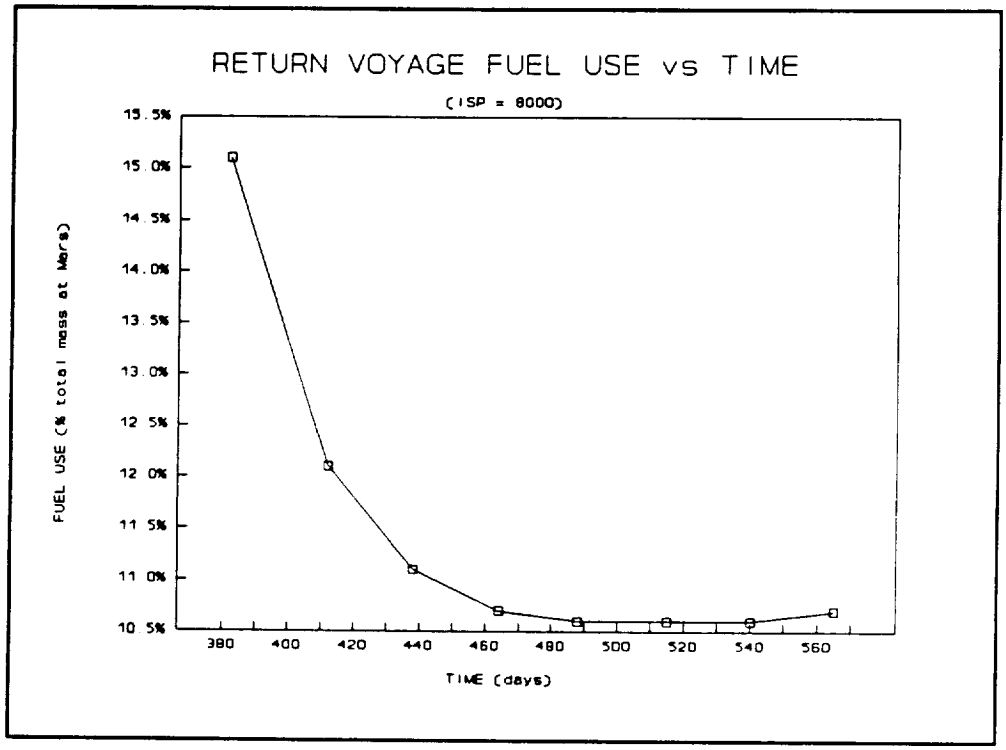

FIGURE 2-4

Once the time of flight and fuel use were obtained, thrust time was considered in order to determine the effect of trip time upon required thruster redundancy. The plot of thrust time vs trip time closely followed the fuel use plot, to which thrust time is directly related. Thus, in minimizing fuel use, a secondary effect of reduced thrust time allowed us to lower thruster redundancy.(see Figures 2-5 & 2-6)

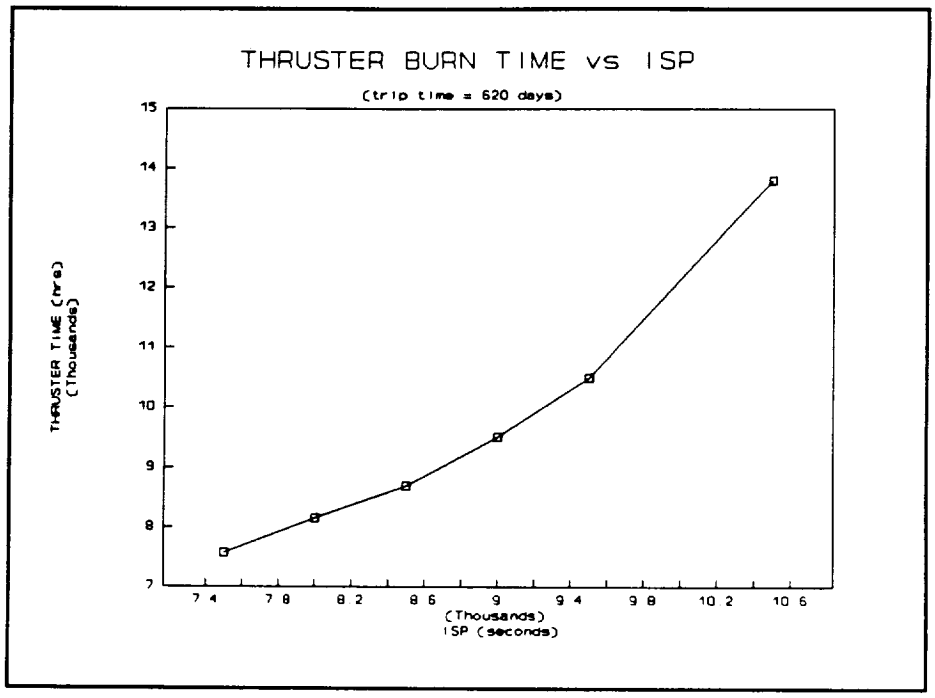

FIGURE 2-5

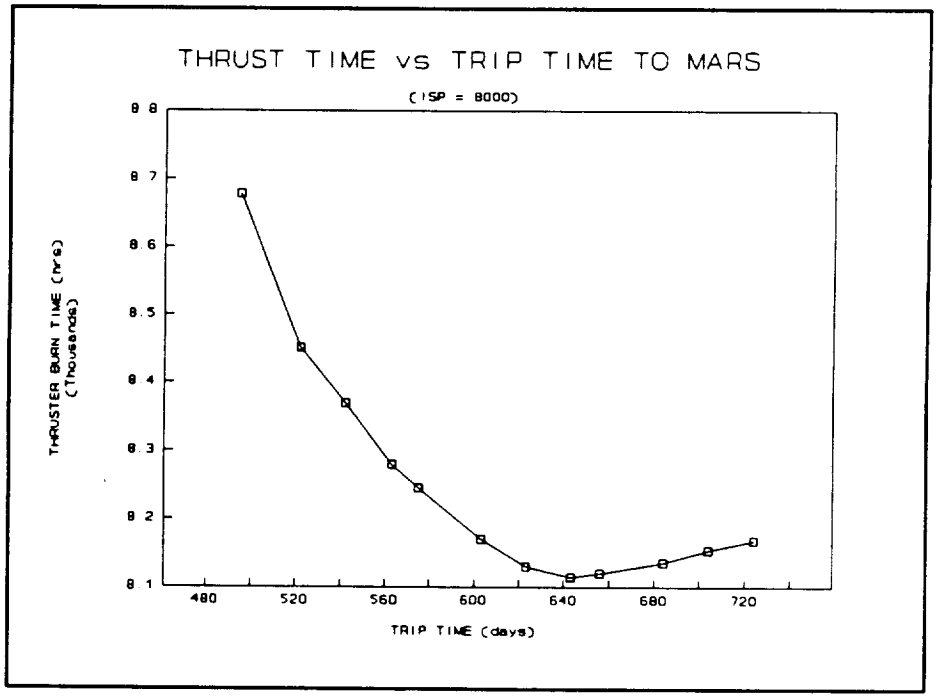

FIGURE 2-6

Using the revised mass estimates, an overall mission time of flight vs Isp plot was developed (Figure 2-7) for the 3MW power near Earth and an Isp of 8000 sec. Note that this curve is a function of many variables: with a constant initial mass, a higher Isp usually involves a longer voyage; but it also requires less fuel, which lowers initial mass and increases thrust acceleration. These varying factors result in a minimum trip time occurring at an Isp of about 8000 sec.

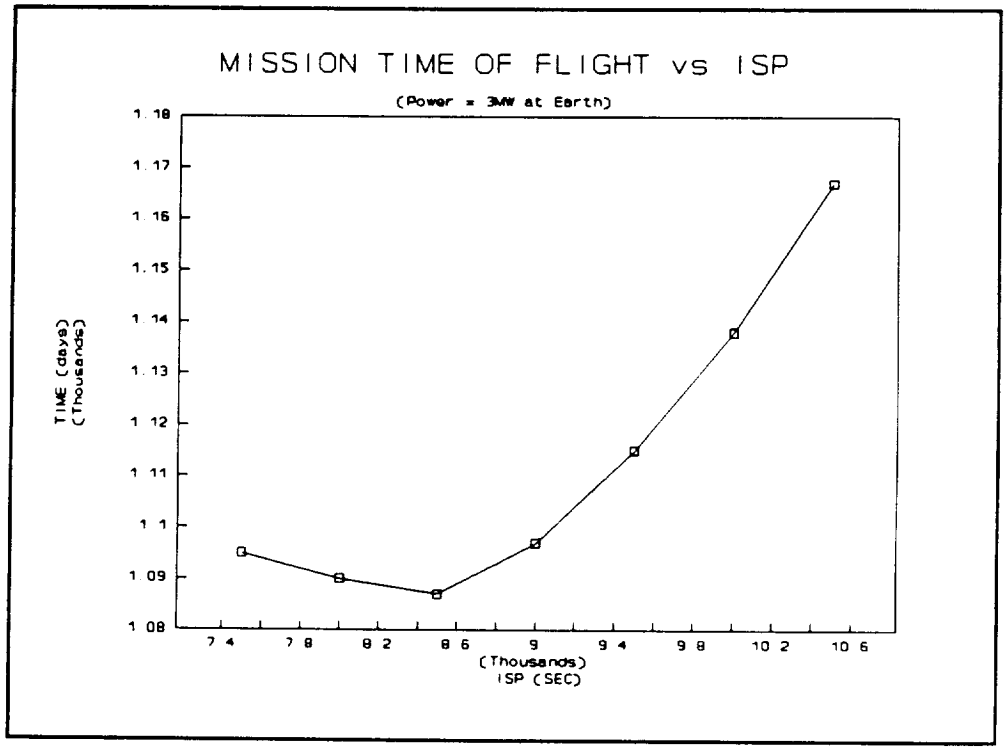

FIGURE 2-7

The 70° inclination change at Mars is accomplished during the Mars capture spiral. When the vehicle reaches an altitude of around 350,000 km, it reorients its thrust direction perpendicular to its orbital plane. It takes about 31 days for the vehicle to move 70° in longitude. The thrust direction is then moved back into the orbital plane and the vehicle continues to spiral down until it reaches 500 km altitude, where it holds in a loiter orbit and deploys the cargo. A similar plane change maneuver on the return trip will require 15 days of thrusting in the out-of-orbit plane direction.

2.2a LAUNCH DATE OPTIMIZATION

In order to optimize fuel use and trip time, the proper launch date had to be established. QUICKTOP allows for this by accepting an initial guess for launch date, and the associated orbital ephemeris, and returning an optimized launch date. To find initial guesses for dates, a spread of four years (2010-2013) was studied using several dates within each year. The best results were considered for the second half of the mission.

To determine the date for departure from Mars, the arrival date was used as an initial guess for the departure date. This was repeated until the desired trip time and fuel use was returned. Using this process, a launch date of May 7, 2012 was found to be optimal over the four year span(33). A launch window of 48 days was calculated using the following criteria:

1) The original fuel use would not increase by more than 5%
2) Trip time would not increase by more than 25 days.

The loiter time at Mars was a direct function of the optimum launch date from Mars calculated by QUICKTOP, with the loiter time simply being the difference between arrival and departure.

RESULTS

PHASE	TIME (days)
1 Earth Escape	161
2 Heliocentric Spiral	401
3 Mars Capture	92
TOTAL (Earth-Mars)	654
4 Mars Loiter	19
5 Mars Escape	68
6 Heliocentric Spiral	302
7 Earth Capture	109
TOTAL (return)	479
TOTAL MISSION TIME	1133 days = 3.1 years

TABLE 2-1 MISSION TIME

The propellant mass required for a round trip was found to be 19,865 kg. A large 20% contingency is added for reserve and auxiliary propulsion resulting in a mass of 23,840 kg. A schematic of the SEMM1 trajectory is shown in figure 2-8.

2.2b DISCUSSION

The results obtained from QUICKTOP were much more accurate with respect to time and fuel use than our initial estimates (based on TRAJ program). The mission time of 3.1 yrs fell just within our design goal and the payload ratio of about 0.5 for a cargo mission is quite good. In comparison to the initial results, the heliocentric times differed by only 13 days. The disparity arose from TRAJ's inflated spiral escape and capture times.

EARTH & MARS POSITIONS — PHASE

E0 & M0 -- BEGINNING OF EARTH SPIRAL

E1 & M1 -- BEGINNING OF HELIOCENTRIC SPIRAL

E2 & M2 -- BEGINNING OF MARS SPIRAL

E3 & M3 -- REACHES LOW MARS ORBIT

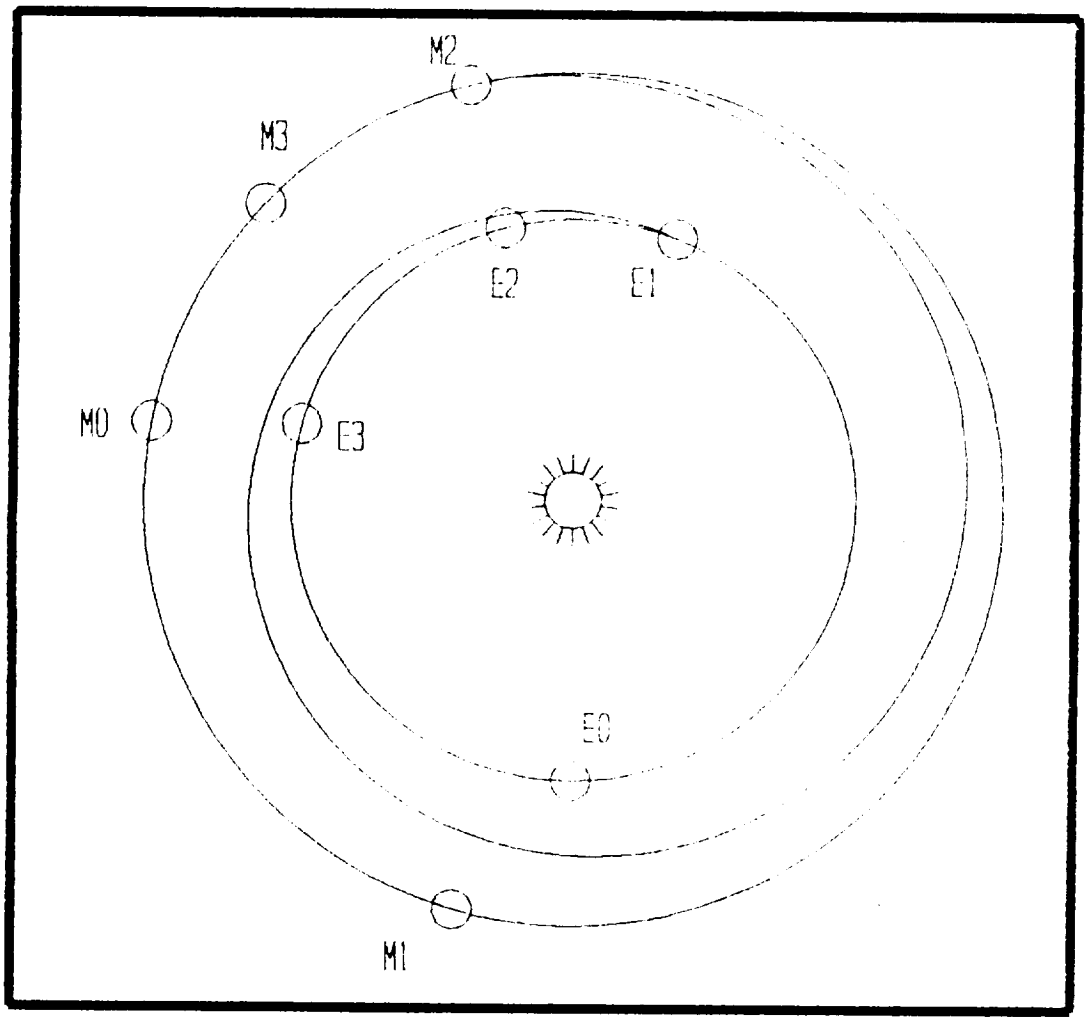

FIGURE 2-8

3. PROPULSION SYSTEMS

3.1 PROPULSION TRADE-OFF ANALYSIS

When designing thrusters, two of the main considerations are specific impulse and fuel requirements. Using a high specific impulse generally means that thruster efficiency is increased and fuel consumption is decreased, but the penalty is that trip times are increased due to reduced thrust at a constant power level. Initial design requirements specified that the propulsion system for this mission should be an argon ion engine run on solar electric power. The results from the solar electric power investigation resulted in selection of the flat panel solar arrays.

Figure 3-1 shows the schematic of an ion engine.

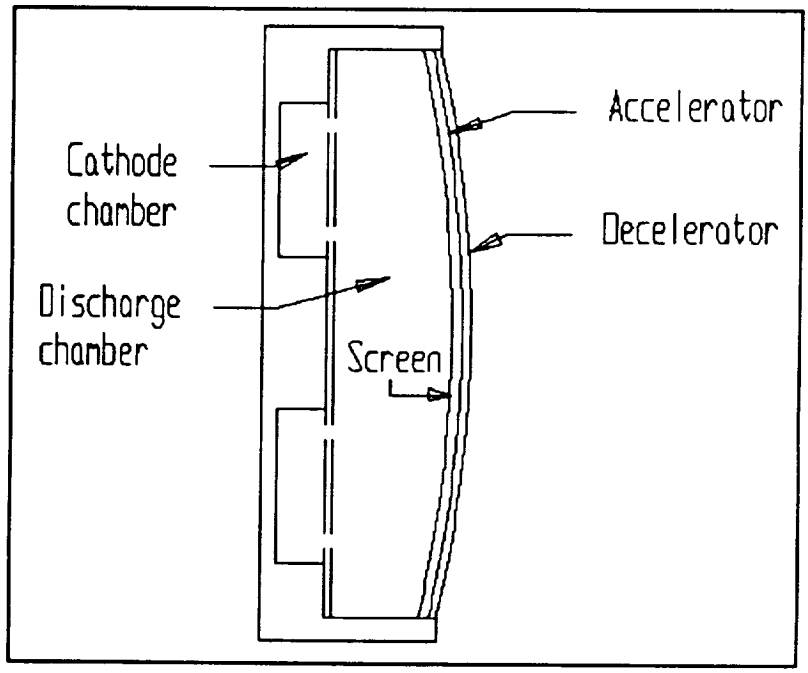

FIGURE 3-1

For about 60 N of thrust at Earth it was found that 3 Mwe of effective power is needed for the thrusters, at a specific impulse (Isp) of 8000 seconds and an initial vehicle mass of 120,000 kg. These findings were the results of an approximate design optimization investigation. In the investigation, various effective powers (Peff) were assumed and analyzed across a wide range of specific impulses. From the effective power and Isp, thruster efficiency (Nth), total vehicle thrust at Earth and propellant mass flow rate were calculated. Next, an iterative process involving

total initial mass (Mi) was utilized to determine the number of thrusters, trip times and masses of propellant, solar power system, structures, fuel tanks and engines. From these masses an iterative Mi was found.

Initially, 30 cm and 50 cm diameter argon thrusters were considered because they have been the subject of many investigations. However, on the basis of recent literature(27,28) it was projected that larger thrusters would be more adequate for our mission. Table 3-1 shows that larger diameters are projected to have higher propellant utilization efficiencies. As a result, further work has been recently done on larger diameter thrusters with diameters greater than 1 meter. Though the quantity of information on thrusters of this magnitude is much more limited than that for smaller thrusters, extrapolations were made for the missing specifications to simulate rough estimates. The major design considerations in our case are the number of thrusters needed, thruster system mass, and cost. The number of thrusters needed for the trip depends, of course, on the size and output of the thrusters. Table 3-1 also shows the changes in output with respect to size(28). The specific impulse is 8000 sec.

Thruster size (cm)	30	50	100	200
Thruster output (N)	0.3	0.8	2.4	6.7
Propellant Utilization	0.855	0.890	0.913	0.929

TABLE 3-1 ARGON THRUSTERS

Thruster lifetimes of ion engines are not significantly dependent on size(27). Some optimistic estimations have predicted 30,000 hour engine lifetimes for small thrusters in the near future(5). From the available data, trends show that there is a decrease in mass due to large diameter thrusters.

The approximate optimization process consisted of the previously mentioned iterative scheme and a tedious balancing of design characteristics. The relationship between thrust and Isp shows that smaller specific impulses yield larger, and desirable, thrusts. However, small Isp's have an adverse affect on the initial mass (Mi). Figure 3-2 illustrates the decrease of mass with increasing Isp.

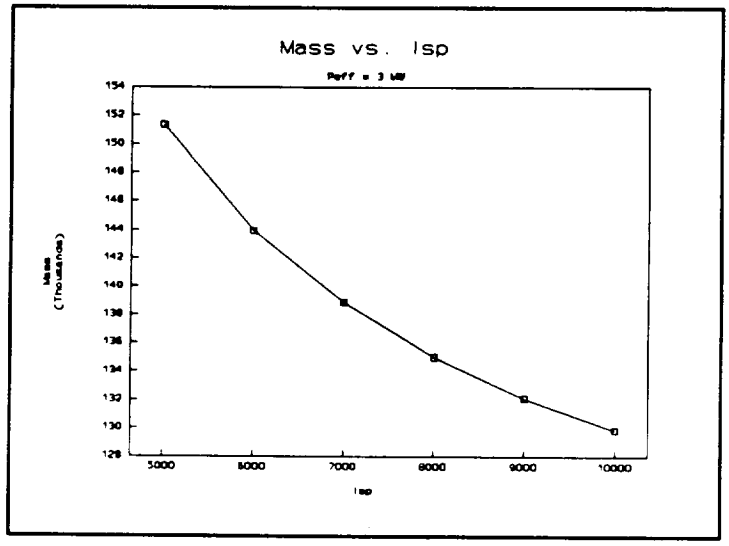

FIGURE 3-2

As a consequence of the reduced initial mass, the payload ratio (payload to initial mass ratio), which is essential to mission efficiency, increases with Isp. This is illustrated in figure 3-3.

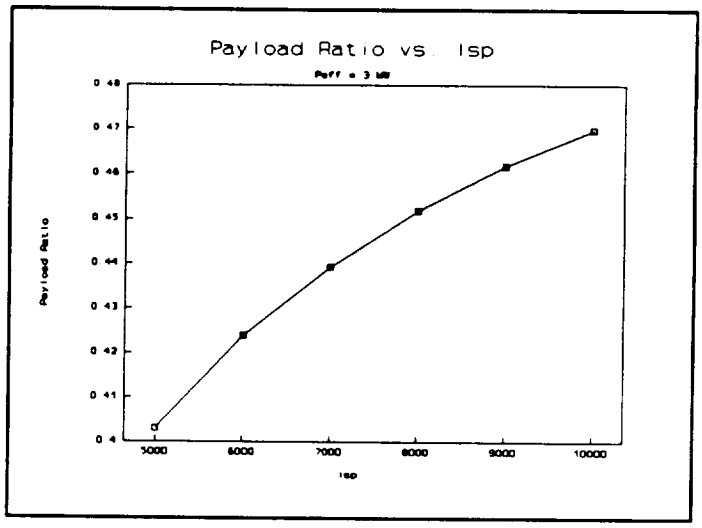

FIGURE 3-3

A range of 5000 to 9000 seconds for Isp was found to be advantageous in terms of trip time. The final design consideration was the number of thrusters required. It was found that for all size thrusters, the number of thrusters necessary for maintaining a maximum thruster efficiency decreases with increasing Isp. Figure 3-4 shows increasing thruster efficiency for increasing Isp.

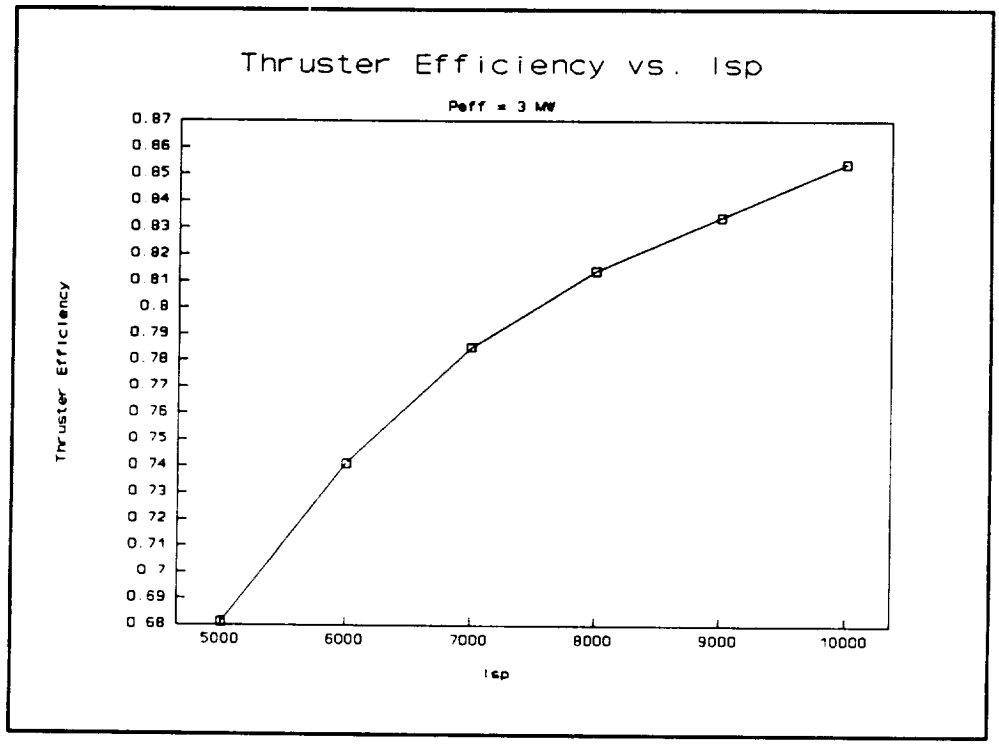

FIGURE 3-4

From this analysis it was determined that a high Isp would be needed for the most efficient vehicle. Once this was concluded, the analysis was carried out for varied effective powers.

Early in the design process, it was found that a range of effective powers from 2.5 to 3.5 MWe would be needed to provide the proper thrust for the mission. The effective power is related to the total power collected by collector efficiency. Increasing the Peff at a constant Isp increases the thrust and tends to reduce total trip time, but at the same time it increases the mass which increases trip time, and thus may partly cancel the reduction just mentioned. Since the total round trip time was to be limited to approximately 3 years, a proper power had to be chosen. The trajectory program QUICKTOP (obtained from NASA Langley) shows that a Peff = 3 MWe would produce the desired trip time. Using a lower effective power would result in trip times that are too long. A higher effective power would increase

the total initial mass. The resulting increased cost due to the extra weight may not be worth the trip time saved. QUICKTOP also shows that for a Peff = 3 MWe the optimum Isp is about 8000 sec.

The effective power and specific impulse given above yield a thrust of 63 N at LEO. This point is illustrated on figure 3-5.

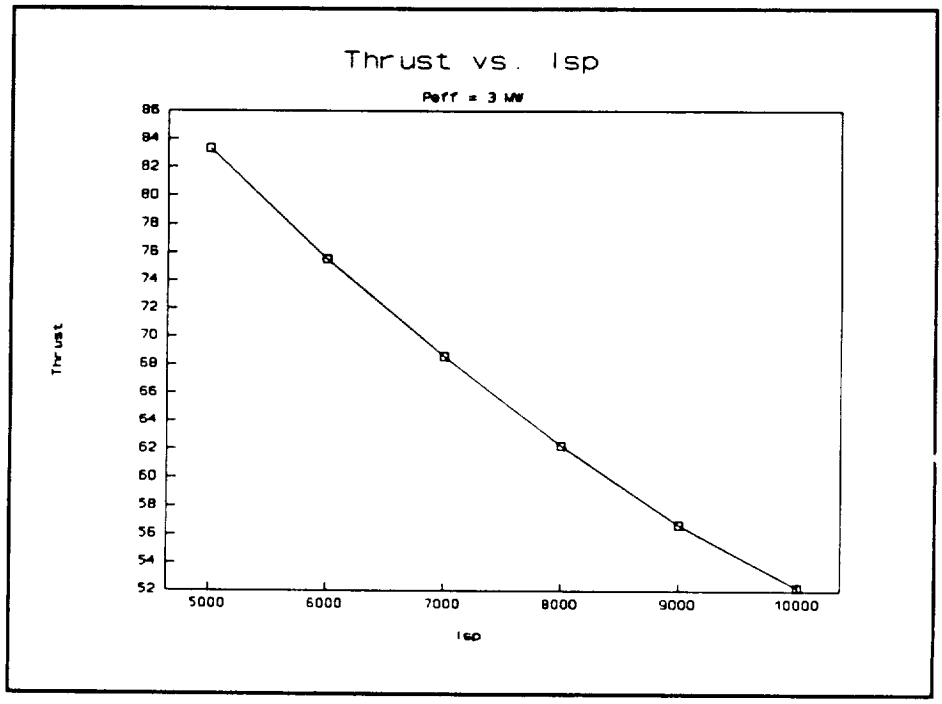

FIGURE 3-5

3.2 PROPELLANT TANKS

There are several variables involved in the design of an electric propulsion tank system. For a chosen propellant, the shape, size and structure of the propellant tanks must be determined, and the pressure and temperature conditions of the propellant itself must be determined. Once these design needs have been met, more detailed criteria must be investigated including thermal control systems and vapor acquisition schemes. This report will center on the propulsion system based on argon propellant because the latter was suggested by the NASA's Space Exploration Office. However, as an added consideration an analysis of xenon as a propellant has been included in section 3.4.

The first step in the SEMM1 propulsion system design process was to choose between cryogenic and supercritical storage of the argon propellant, table 3-2 shows a comparison of the two states.

Argon	Temp (K)	Press (atm)	Specific Volume (m_3/kg)
Cryogenic	85	1	7.04×10^{-4}
Supercritical	>151	>48.1	2.996

TABLE 3-2 STORAGE COMPARISON

It can be seen that the supercritical storage requires a much larger volume and pressure. Such demands yield a significantly greater tank size and mass than the cryogenic storage. This critical fact forced the selection of argon in a cryogenic state.

The next step in the design process was determination of tank structure and shape. Two basic types of tanks were analyzed: elliptical and spherical, or cylindrical, tanks. It was found that ellipsoids yield optimal tank shapes for cryogenic propellants. Ellipsoidal tanks are structurally sound and provide a simplified vapor acquisition system at a cost of increased fabrication complexity. The vapor in the propellant tanks must be extracted from a vapor bubble that is formed in the tank. In an elliptic tank the vapor bubble moves to the part of the tank that has a maximum diameter. Thus the vapor bubble is always located in the same place and vapor acquisition is simplified. The tank system itself may consist of two shells, one inside the other. The outer shell with insulation would serve as a radiation shield and the inner would act as a pressure vessel. Thus, the shells may be separated by argon

vapor piped from the inner tank that would act as a coolant for the pressure vessel. Such a cooling system was found to have negligible propellant losses(10). This configuration can be seen in Figure 3-6.

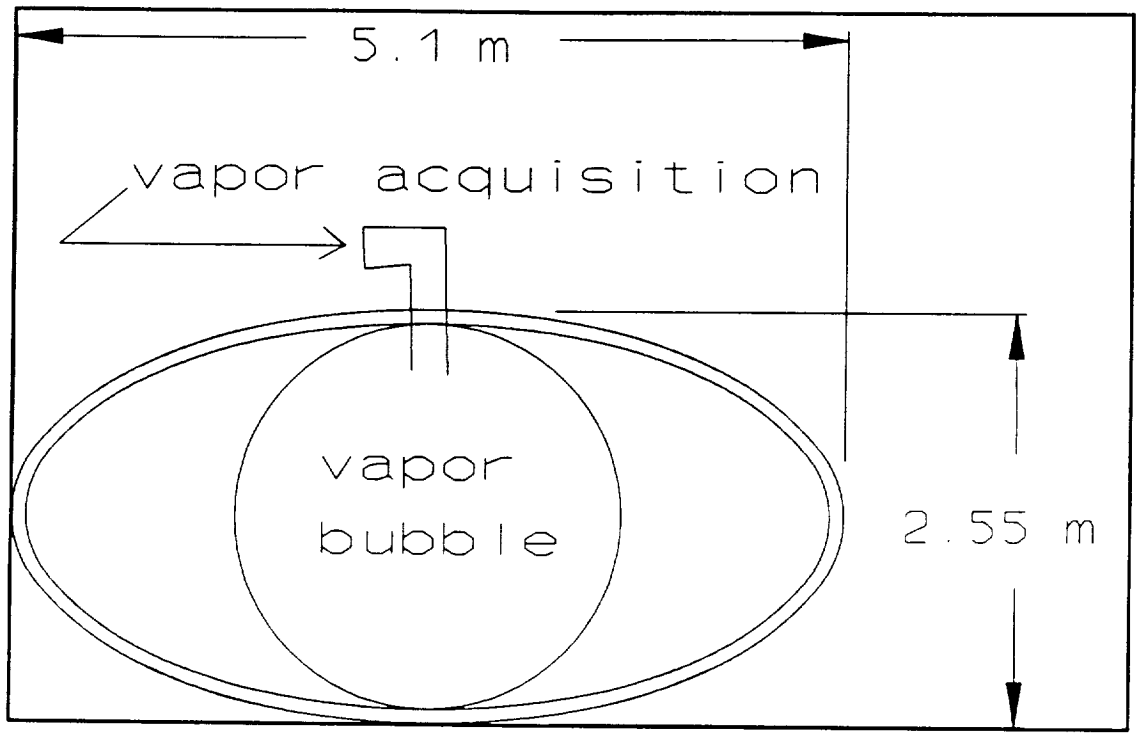

FIGURE 3-6

A collapsible bladder tank has also been investigated (figure 3-7). While such a tank may yield a 97% expulsion efficiency, its disadvantages include large tank volume to contain an all-vapor phase fluid and a requirement for an additional gas to expel the propellant. These two facts make the CBT's quite inefficient for our project. Cryogenic elliptical propellant tanks were found to be the preferred configuration for SEMM1.

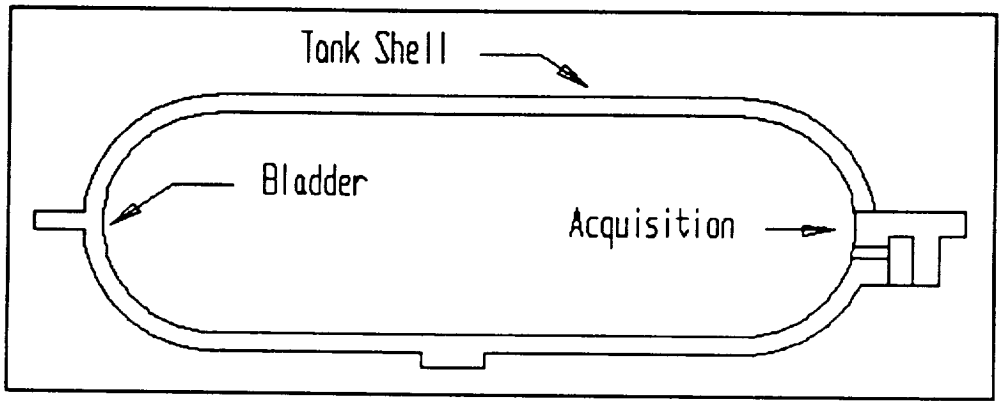

FIGURE 3-7

A single ellipsoidal tank for cryogenic argon storage was selected. Figure 3-6 shows the dimensions of the tank and table 3-3 provides specifications for argon storage.

Total Propellant Mass	23,840 kg
Total Volume	17.3 m^3
Temperature	85°K
Pressure	1 atm
Density	1420 kg/m^3

TABLE 3-3 ARGON STORAGE

The argon vaporized by solar radiation incident on the tanks will be piped out of the tank and sent to the thruster system. In addition, some of the vaporized propellant will be sent between the two shells of the tanks to cool the remaining argon. The vapor probes used to extract and transfer the vaporous argon will be constructed of composite ceramics due to their high strength combined with a low thermal conductivity. The tank thermal control system consists of multilayer film and honeycomb insulation, composite films and paints for the outer surface, and heating coils to maintain the vaporization of the argon near Mars. The need for thermal

control stems from the requirement to keep the propellant flowing at the desired rates at the Earth and Mars orbits. In addition, since solar absorbance increases with the life of the mission, due to the continuous contamination and attacks of charged particles and ultraviolet radiation, there is a need to provide the tanks with adequate protection. The tank shells will be constructed of thin aluminum-lithium alloy. The meteoroid/debris protection and thermal insulation of the tank will consist of surface coated (with Kapton H and inert oxides) face sheet (Gr-Polyimide), spacer material (low density foam or fiber wool), intermediated reinforcement (Kevlar cloth) and 120 layers of MLI (multilayer insulation). The latter consists of layers of low conductivity materials such as dacron polyester tuft loc, sandwiched between highly reflective metallized polymeric films. The total thickness of the meteoroid/debris protection and thermal insulation is about 16 cm.

The propellant tank will be encased in a box like structure. The dimensions of the housing take into account the piping and structural material of the tank. The tank will be refueled and/or replaced after every trip. The tank housing is connected to the thruster module in such a fashion that allows for quick connection of fuel lines as well as easy maintenance access. The interface between thruster and tank modules is displayed in Figure 3-8.

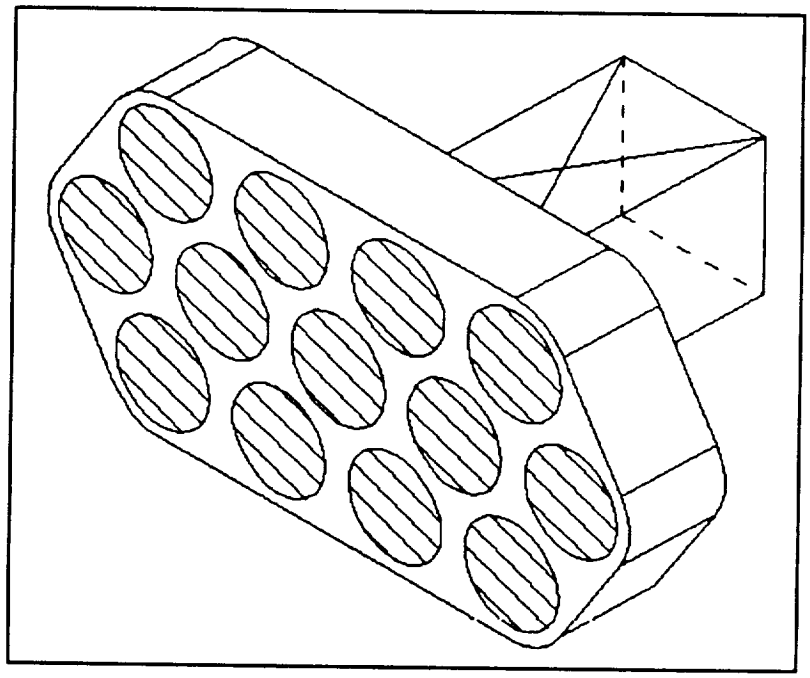

FIGURE 3-8

Near Earth, 10 thrusters are used and the propellant mass flow rate is 7.65×10^{-4} kg/s or 120 W of heat to vaporize the liquid argon. This heat is provided by the thermal energy penetrating the tank insulation and by the heating coils inside the pressure shell. As the surface tank temperature near LEO is about 330 K and the

MLI conductivity can be assumed about 1.8×10^{-5} W/K-m, the heat penetrating the MLI will be around 2 W. When the craft coasts and the thrusters are not in operation, the vaporized argon will be refrigerated by a small (about 60 W) Stirling refrigerator. The mass breakdown of the tank system is given in Table 3-4.

Tank Shells	240 kg
Debris/Meteroid Protection/Insulation	210 kg
Refrigeration subsystem	120 kg
Electrical heaters, sensors, controls	80 kg
Propellant lines, valves, regulators	200 kg
Total Mass	850 kg

TABLE 3-4 MASS BREAKDOWN

3.3 THRUSTER SYSTEM

The selected propulsive system consists of 13 argon ion engines in a modular thruster unit that is easily serviced and maintained. The modular design is presented in figure 3-9 (on the next page). The engines can be removed separately or the whole unit can be pulled. The entire thruster system unit will be launched from the Earth's surface. Table 3-5 shows the scheme for thruster utilization. The thruster numbers refer to corresponding numbers in figure 3-9.

Orbit Phase	Thrust (N)	Number of Thrusters	Thruster Numbers
Earth Spiral	58 - 60	10	1-5,9-13
Heliocentric Spiral	52 - 54	9	1,4-10,13
	46 - 48	8	2,3,5,6,8,9,11,12
	40 - 42	7	1,4,5,7,9,10,13
	34 - 36	6	2,3,6,8,11,12
Mars Spiral	25 - 30	5	1,4,7,10,13

TABLE 3-5 THRUSTER UTILIZATION SCHEME

Engine size and parameter have been selected on the basis of ion thruster calculations (55) and results published by ion propulsion investigators (27). The key requirements driving selection of engine design and parameters were: (a) large beam diameter to limit the number of engines and (b) beam power per unit area and net-to-total accelerating voltage ratio (R-ratio) selected so as to minimize ion defocussing and grid erosion as well as backstreaming of the neutralizing electrons. These requirements were in addition to the previously discussed selection of a high specific impulse to minimize propellant mass.

Table 3-6 shows some of the pertinent characteristics of argon ion engines at an Isp = 8000 sec.

Thrust per engine	= 6 N
Beam diameter	= 2 m
Power input per engine	= 306 kW
Beam current	= 190 A
Net Voltage	= 1477 V
Grid gap	= 3.33 mm
Chamber length	= 0.423 m
PPU efficiency	= 0.95
Thruster efficiency	= 0.814
Propellant utilization	= 0.929

TABLE 3-6 THRUSTER CHARACTERISTICS

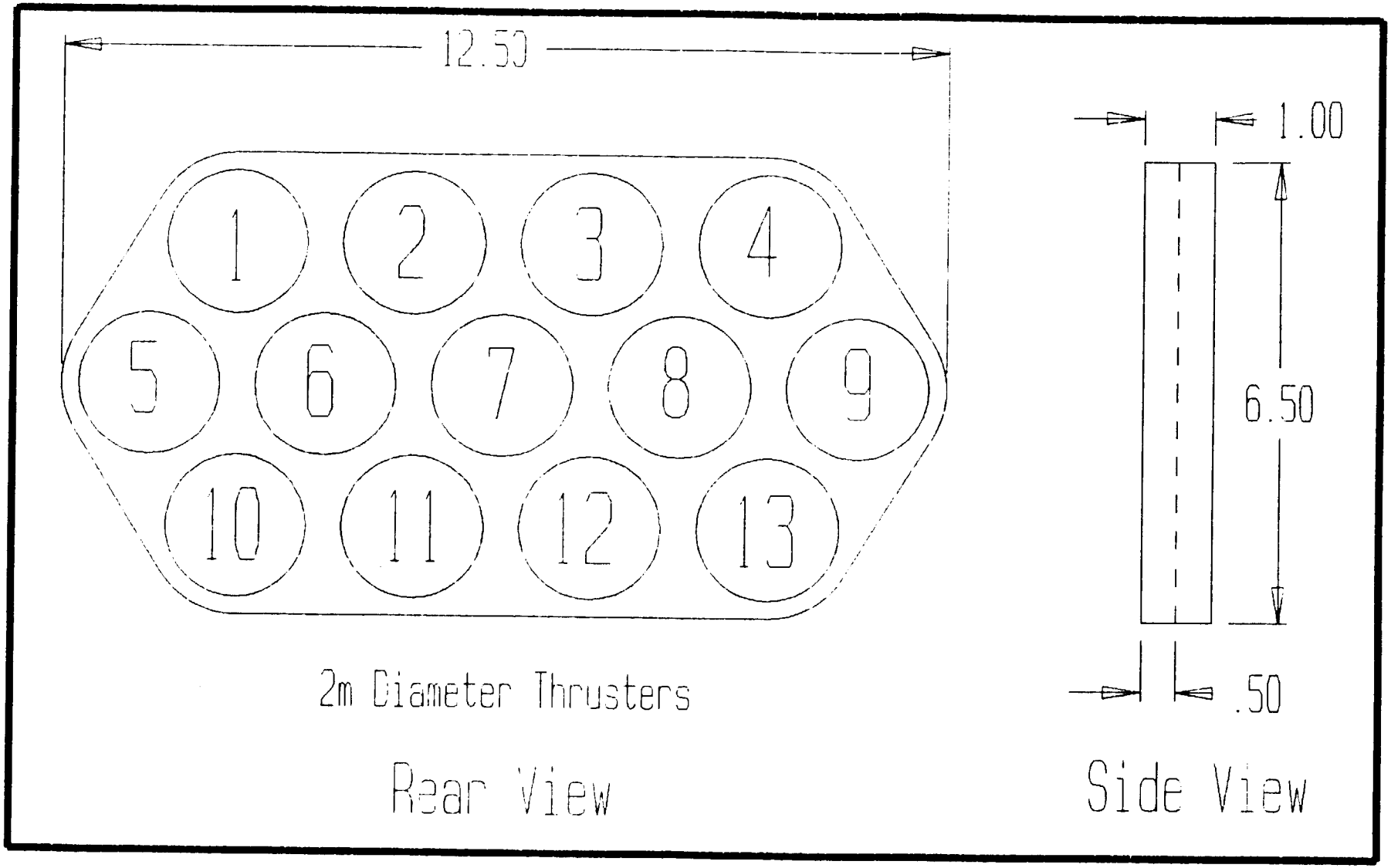
12.50
1
2
3
4
5
6
7
8
9
10
11
12
13
2m Diameter Thrusters
Rear View
1.00
6.50
.50
Side View

FIGURE 3-9

The projected lifetime of the thrusters is approximately 25,000 hours. No thruster should exceed its lifetime during the mission, but a 30% redundancy has been included for a case of thruster malfunction or burn out. Ten thrusters will be operational at LEO to achieve the desired thrust output. The onboard navigational computer will periodically shut down thrusters during the trip out to Mars to make sure that thrusters are run at full power. This is because the thrusters loose efficiency when they are not operating at full power(45). Computer software integrated with the navigational computer will manage the thrust vector as well as make sure that each engine gets nearly the same operating time. This will minimize the chance of exceeding the expected engine lifetime.

The output from the solar arrays must be conditioned to the form required by the argon thrusters. The Power Processing Unit (PPU) consists of input filters, transformer coupled inverter (DC-AC) followed by regulated power supplies for discharge/cathode, neutralizer, screen and accelerator. The unit must include provision for switching, restart and high voltage fault clearing. The heat generated by the electrical components will be dissipated to space by an advanced radiator based on a carbon-carbon composite pumped loop radiator design(54). With heat rejections at 600 K, the radiator size will be about 75 m^2 (emissivity 0.8).

Mass estimates of the power conditioning and radiator systems have been based on the current projections derived from the studies initiated by NASA and the SDI office. These projections range from 1.2 to 2.5 kg/kWe, for the megawatt power range.

Thrusters (13 x 490kg)	1820 kg
PPU and Radiator	7100 kg
Gimbals, housing structure, engine sensors and start-up controls	650 kg
Total Mass	9570 kg

TABLE 3-7 PROPULSION SYSTEM MASS SUMMARY

4. POWER GENERATION AND DISTRIBUTION

Sending a cargo ship to Mars and back requires a large amount of energy. In addition to the main ion thrusters, the ship requires many auxiliary components such as motors, gyros, computers, sensors and communications gear. The power that is fed into the ship must be divided and conditioned into distinct, useful electricity, then distributed to every piece of machinery on board.

Solar power was selected as the method of producing power for this mission, but there are many types of cell materials and several different power collection systems that merit consideration. The array has to be lightweight. The array has to have a high efficiency in converting sunlight to electricity, or the area of the array would be very large. Although area is not a limiting factor in itself, the packing requirements and structural stability dictate that the size be given careful consideration. Lastly, the array has to operate in an environment of radiation without degrading to such an extent that the mission would be jeopardized. These goals can be met by a combination of technology from two separate areas; cell materials and array configurations.

4.1 SOLAR CELLS

A photovoltaic element is a semi-conductor that emits free electrons when bombarded by photons from a light source. Therefore, electricity can be drawn from these elements when light from the sun falls on them. This is a very clean, safe way of making power, and there are many advances being made in this field of technology.

The first elements to exhibit the photovoltaic characteristics were silicon cells. Many years of study have produced reliable solar cells from silicon, but recent advancements in other cell materials have produced far more exciting results. Gallium Arsenide (GaAs) has been shown to be much more efficient than silicon, and more radiation resistant. While silicon has the theoretical potential to reach an efficiency of 18%, GaAs can achieve up to 24%(18). This can be seen in the Figure 4-1.

The development of Indium Phosphide (InP) cells and multi-bandgap cell combinations opened new doors for space power systems. InP is a cell material with a potential efficiency of 23%. However, interest in this type of cell stems from its ability to repair its own radiation damage. Multi-bandgap cells are combinations of two or more cell materials with different photon absorption properties. The atoms in each cell material will absorb photons and reradiate electrons at only one certain energy level. The remainder of the unabsorbed photons usually pass right through a single cell. With two or more cells, as seen in Figure 4-2, the photons that got past the first cell are mostly absorbed by the bottom cell, thereby increasing the material's efficiency(18).

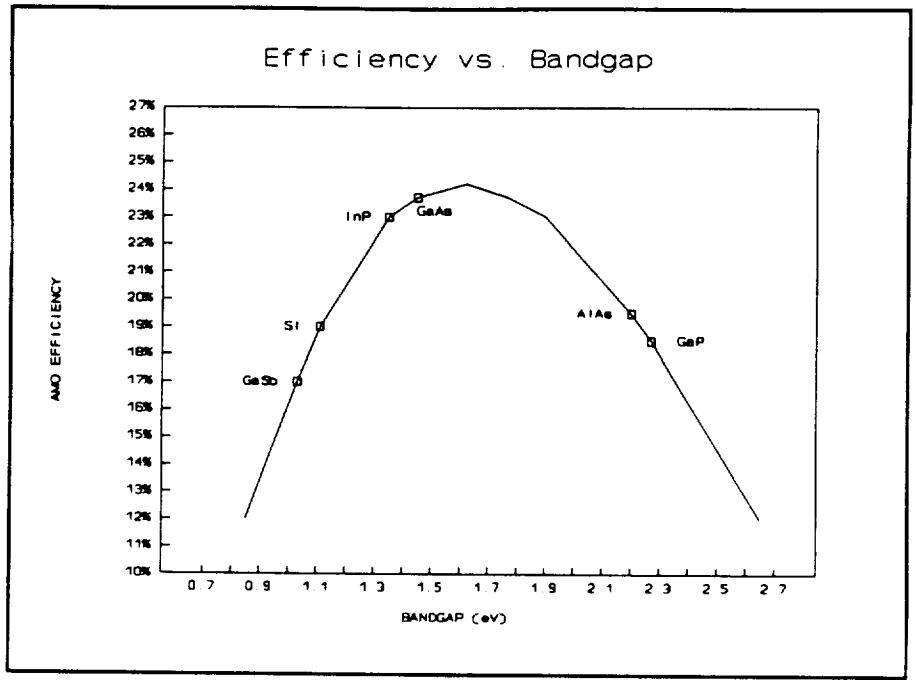

FIGURE 4-1

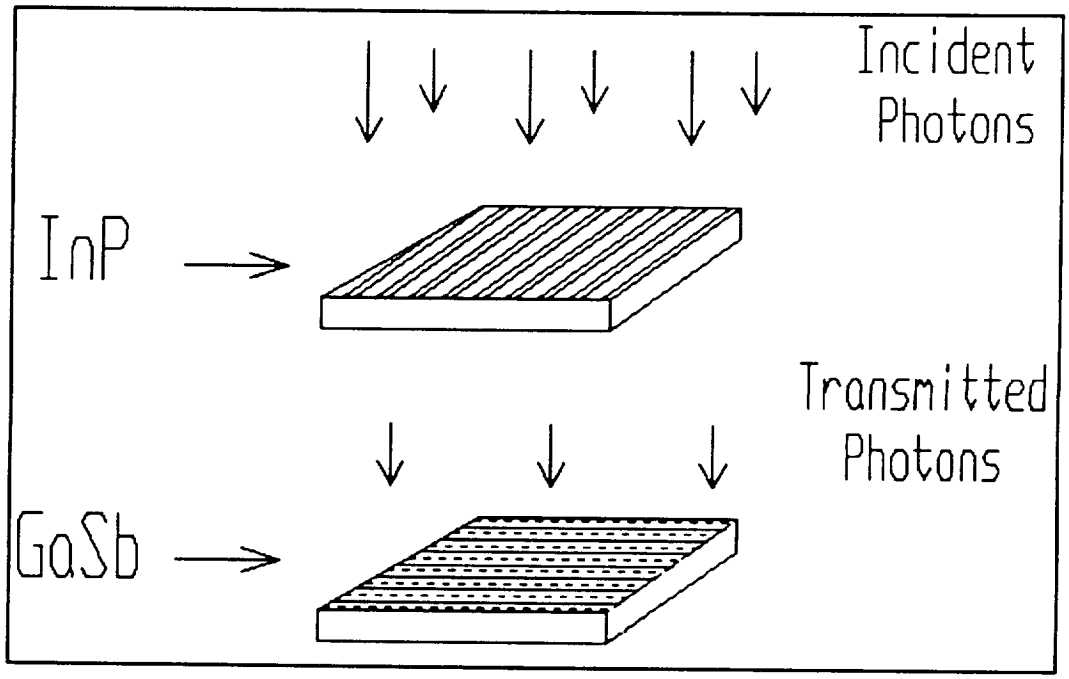

FIGURE 4-2

4.1b Radiation Damage

Photovoltaic cells operate with great sensitivity to fluctuations in the presence of charged particles. Exposure to free electron and proton radiation can damage the cell material, even to the extent of total loss of power production. Around Earth, there are particles from cosmic and solar radiation that are trapped in magnetic fields, forming the Van Allen belts. These belts are a major obstacle to the Mars mission, which requires a very slow spiral outward from the LEO.

Normal solar cell materials will experience degradation on the order of 20-30% of their Beginning of Life (BOL) power(31). This reduction would force the ship to carry oversized solar panels in order to provide adequate power after a three year journey through space. These panels would also have to be replaced between every mission, producing an enormous waste of money, time and material.

A promising solution came by considering the use of InP. The normal radiation resistance of the wafer has been shown to be stronger while it is being illuminated by sunlight, no matter how intense. In addition, experimentation has demonstrated that an InP cell exhibits self-annealing from electron-induced radiation damage when held at a temperature of 100 degrees C for any length of time(18). In fact, in about ten minutes at that temperature, the cell can completely recover its power producing abilities even after having been reduced to zero electrical output by radiation degradation. Assuming that this fact would hold true for proton damage as well, a radiation hard solar array can be manufactured that would last almost indefinitely, regardless of how often or how long it is used.

Recent reports have shown that a p/n junction indium phosphide cell can achieve an efficiency of over 22%. Current optimum cells use n/p structures because they produced the best results in early experiments. However, Rhoads and Barnett (40) presented a model for a p/n junction device that has predicted new designs for high voltage, high efficiency InP solar cells. This new design exploits the high absorption capabilities of InP, as well as its relatively long diffusion lengths and modest surface recombination characteristics. This cell uses a very thin emitter layer with a high doping concentration. Doping is a process of impurifying the semiconductor to enhance the electrical behavior of the cell.

4.1c SEMM1 Cell Materials

The multi-bandgap solar cell for the cargo ferry will use a p/n junction InP top cell with an open circuit voltage of 928 mV and a short circuit current of 38.2 mA/cm^2. The efficiency of the InP evaluated at air mass zero (AM0) is 22.5%. The characteristics of the 5 x 5.4 cm cell are summarized below.

emitter:	thickness	.02-.07 micrometers
	doping	6E+17 $1/cm^3$
base:	thickness	5.0 micrometers
	doping	6E+16 $1/cm^3$

The solar cells will be of a multi-bandgap type, using InP as the top layer and gallium antimonide (GaSb) as a bottom cell. This combination has been studied and experimented with at Boeing and Entech (38), who used the cell in their mini-domed Fresnel lens. The GaSb bottom layer absorbs photons of a shorter wavelength than InP, and will add another 8% efficiency to the total capability of the cell. The addition of the GaSb bottom cell changes the cell output to 48.2 mA/cm^2 and 714 mV. Operating at high temperatures, however, tends to reduce the cell's efficiency on the order of 4-5%. Losses will also occur due to packing factor, wiring, and mismatch. The power conversion system will also reduce the total efficiency slightly. A small amount of current will also be drawn from the main feed to be rerun back through the cells in a forward bias configuration to keep the cell materials above 100° C. Taking into account all of the factors listed above, the effective power from these solar cells is projected to be 303.6 W/m^2.

The cell conversion efficiencies are summed as follows:

Indium Phosphide	22.5%
Gallium Antimonide	+8%
Cell Temp. (100° C	-4%
Total	26.5%

The physical and electrical losses are listed below:

Packing Factor	-5%
Wiring/Mismatch	-5%
Power Conversion	-2%
Forward Bias Current	-1%

The net cell efficiency is projected to be about 22% near LEO, resulting in a net power output of 3,148 kW.

The losses to be expected after the Mars journey include:

Abrasions/Clarity	-1%
Impacts/Malfunctions	-1%
Irreversible Degradation	-1%

The InP/GaSb cell will be bonded by an adhesive and sandwiched between the cover and substrate. The top layer is a cell cover, designed for protection and to eliminate losses due to obscuration at the edges of the cells. An anti-reflective coating will help keep the sunlight from bouncing off the covers and wiring on the blanket surface. The bottom material is a 2-mil thick Kapton polymide substrate. This material is a carbon-loaded dielectric, and its resistivity is such that it serves as a ground to prevent electrostatic charge buildup. The substrate must be treated with a SiO_2 coating that will prevent erosion of the Kapton by atomic oxygen in the space environment(51).

4.1d Evolution of Solar Array Configurations

There are many ways that solar cells can be exposed to sunlight. The traditional flat panel array has been well proven and technology has produced a very lightweight structure. Another approach is to use optical concentrators to focus the sun's light on a smaller solar cell. These reduce the amount of area needed to produce a set amount of power. Double reflective mirrors are popular and well-proven on Earth, but a 12-meter dish would weigh far too much for space power systems. Tiny reflective concentrators have been produced that weigh less, but are still too heavy to be efficient.

Refractive optics has shown to be very promising, using lenses to diffract incoming light and focus it onto a solar cell. Mini-dome Fresnel lenses have been developed and are the center of intense research at NASA's Lewis Research Center(38). The domed concentrators can be manufactured and fitted into a square structure, so that most of the incoming light is captured. These cells operate at 130 C, which would enable a small cell of InP to demonstrate its self-annealing capabilities.

Unfortunately, the Fresnel lens array requires large advances in structural technology. There is work being done at Boeing that promises to make the structure very lightweight by hollowing out the interior walls and using stronger, lighter materials. However, an array that produces 3 MW of electrical power must be huge, requiring the manufacture of thousands of lenses and the painstaking assembly of the box-like structure. In addition, as the array grows in size, its flexibility begins to cause problems, and potential bending can occur at locations far from the ship's center. This would require a beefy support structure for the array of lenses, just to hold it steady, since the lenses can only operate within a sun-pointing tolerance of ± 1 degree. This may be impractical to achieve on an array of this size, and may be difficult to erect in space, unless astronauts were to spend hours constructing it.

The basic flat panel technology is much more usable. NASA has been working on solar panels for its proposed Space Station Freedom for several years, and has flown a few prototype arrays on the space shuttle. These panels were around 30 meters long and about 4 meters wide, and demonstrated adequate stiffness and deployability under space environments(51). These types of panels will form the power system for our ship.

4.1e SEMM1 Solar Array Configuration

The solar array configuration was strongly influenced by three factors: assembly time, launch packaging, and pointing accuracy. Flat solar panels were chosen over Fresnel lenses because the structural strength needed to achieve high pointing accuracy would have added complexity to the assembly and significantly increased the weight of the arrays. Extendable solar arrays are advantageous in that they are lightweight, consist of solar panels which require a lower pointing accuracy, are self deployable, and are compact when stowed. The lower requirement on pointing accuracy allows us to use a single truss to support each arm. These arms will be divided into large preassembled sections that can be put into orbit with a heavy lift launch vehicle.

The ability to have preassembled sections will significantly cut down on costly EVA time. The baseline designs for the Space Station Freedom are being redrawn because the time required for the astronauts to assemble and upkeep the station was enormous. The new configuration is based in part on sending up the truss sections pre-assembled, enabling ground testing of the structure that was previously unavailable. The Mars cargo ferry will take advantage of NASA's decisions and duplicate their efforts. Since astronaut time is much too expensive to be taken lightly, automated deployment and pre-assembled packaging may be more important that simple weight or size constraints.

The power system consists of 24 deployable solar arrays that extend out from a long central truss. The truss is attached to each side of the ship, forming two "wings", with 6 arrays fore and aft, on each wing (figure 4-3). Each array consists of two solar panel blankets that are held in tension by a mast extending between them (figure 4-4). The blankets are 40 meters long and 5.4 meters wide, making them slightly bigger than the prototypes that were flown earlier. The weight of the solar blankets including wiring will be 1.0 kg/m^2. Each mast tip will house a small control moment gyro weighing 8 kg. This gyro will work to keep the blanket array from bending too far under the effects of thrust or docking impact. One axis of stability is sufficient because the acceleration of the ship will always be in that direction. The extendable mast, stowage canister, and stabilizing gyro will account for about 36 kg. This will bring the weight of each deployable module to about 505 kg.

The solar arrays will be anchored to the truss during assembly. Each array is totally independent and is connected to the truss only by its base. The array is self-deployable, and its coilable mast will unwind and lift the cell blanket from its storage box and pull it taut. The mast longerons and battens are made of fiberglass and the diagonals are braided steel cable. Each array is 0.6 meters away from its neighbor, giving it enough room to wobble on its own.

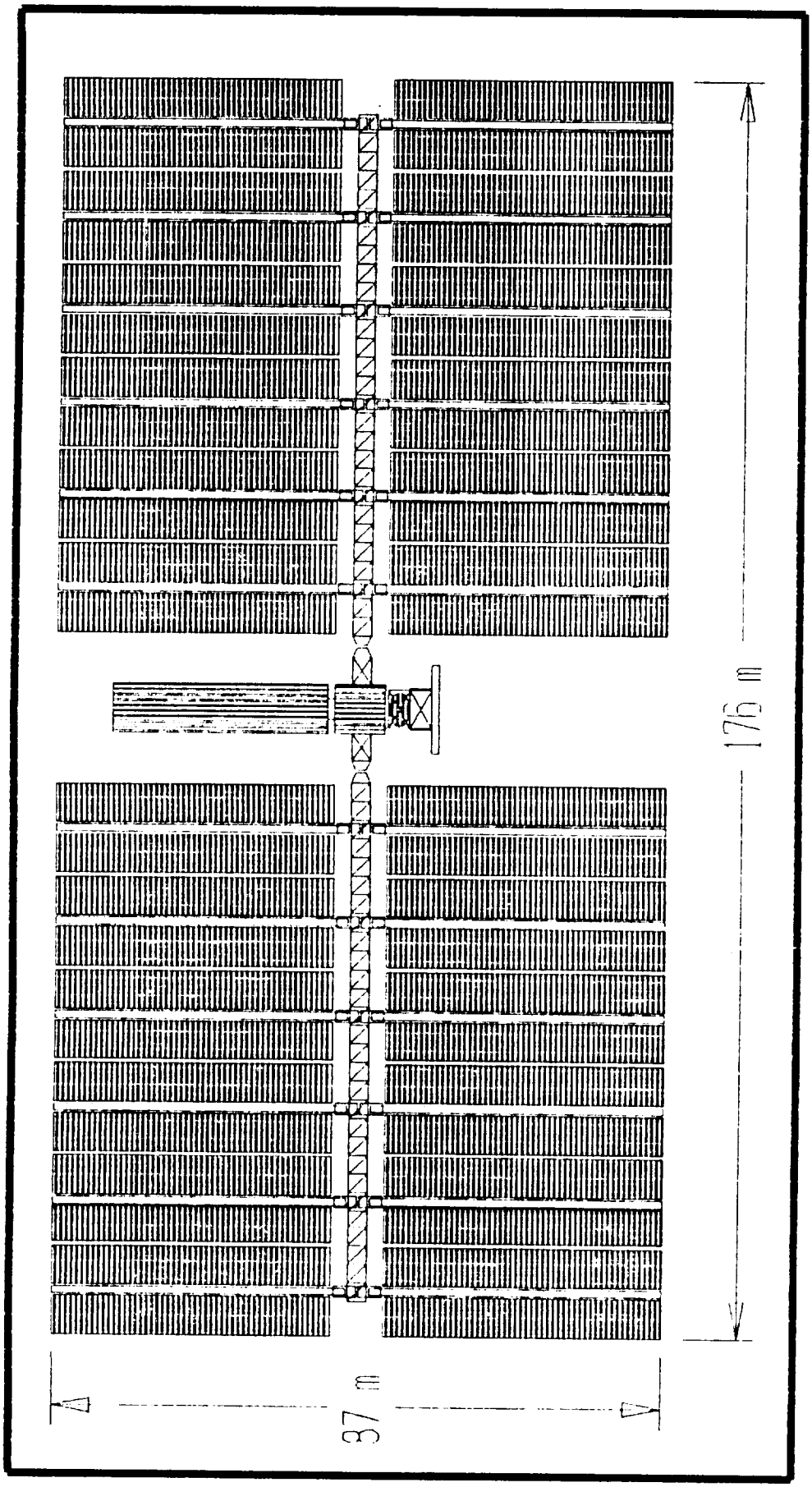

FIGURE 4-3

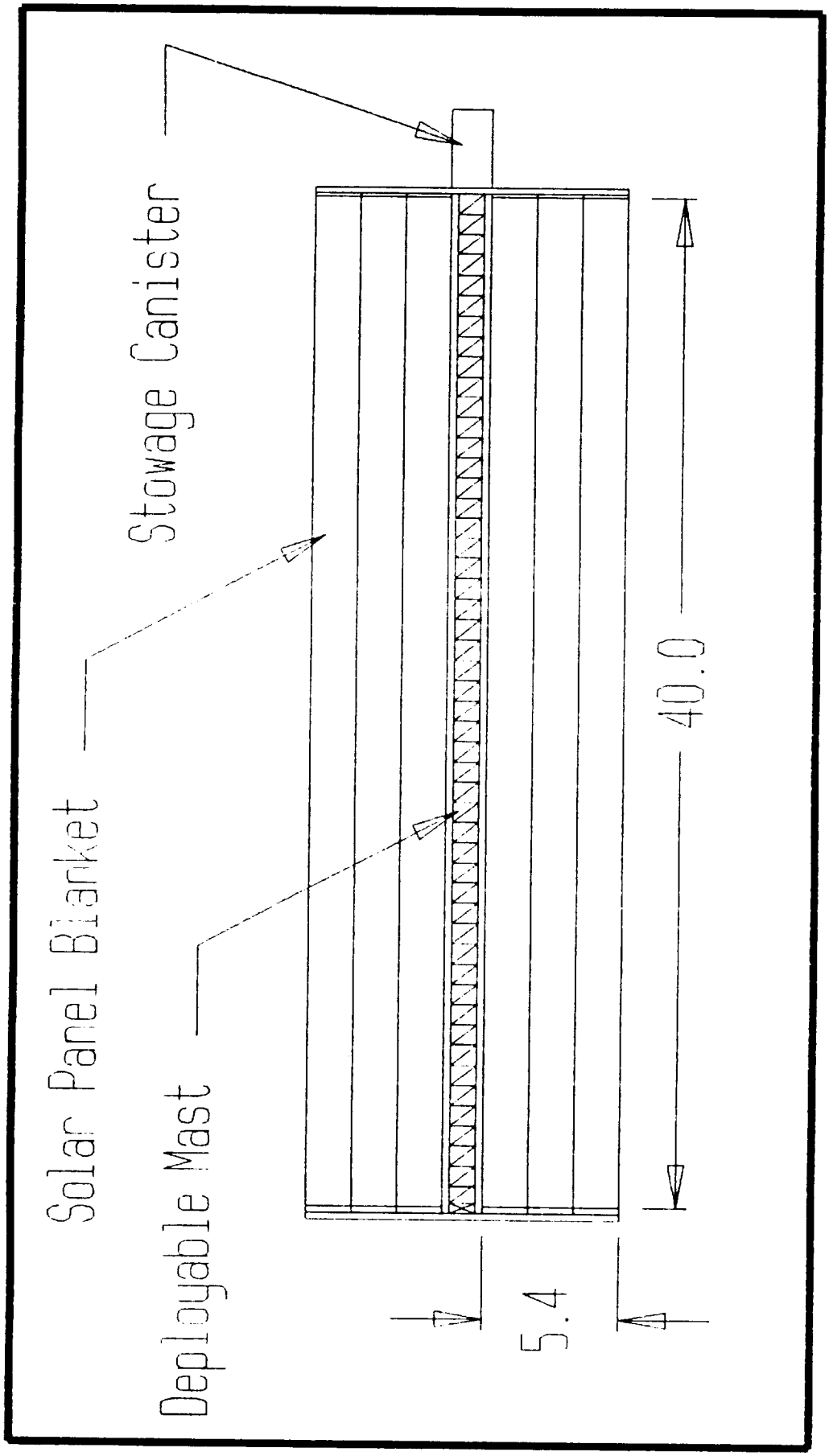
Stowage Canister
Solar Panel Blanket
Deployable Mast
40.0
5.4

FIGURE 4-4

4.1f Stability and Control Characteristics

The flat panel is very forgiving of sun-pointing errors. Since the cells absorb the light which falls directly on them, the sun's intensity will drop off with pointing error as a cosine function. This gives the cells 95% sunlight even if the panel is bent away from the sun by almost 20 degrees. Too much bending can be harmful to the structure, however, so the small control moment gyro is fixed to the tip of each array mast, giving it active control and holding it nearly level. The array has a natural frequency of 0.2 Hz and a stiffness of 0.015 g(51). This is adequate in the space environment, and the gyro ensures that the arrays will never oscillate at resonance.

4.2 Wiring

The solar power is generated by twenty four individual deployable solar arrays. Each of these arrays is 40 m x 10.8 m(solar material only), and is divided in half lengthwise. The wiring scheme for one of these halves is shown in figure 4-5. The individual solar cells are 5 cm long and 5.4 cm wide. The 40 m x 5.4 m section is also divided in half. The two halves shown in figure 4-5 contain 800 rows of 50 cells. In order to avoid creating any sort of magnetic field all wiring will be run symmetrically starting and ending on the outer edge of each side of the array blanket. The cells will be wired in strings of 200 cells, or four rows, in series. This will amount to a line voltage of 142.8 V and a current of 1.263 A for each string.

Cells A, B, and C, shown in figure 4-6 demonstrate the wiring scheme used to wire the strings of solar cells. Because the cells are wired in series some special safety measures have to be taken. If one cell were to be damaged or destroyed by debris or by some other means the current generated by all of the cells "upstream" would be lost. In order to prevent these losses each cell is wired with a reverse bias configuration. Wires 1, 2, and 3 create an alternate path for the current to take if one of the cells should malfunction or become damaged. Each wire is fitted with a reverse bias diode which gives the wires an infinite resistance relative to wire 4 which is the proper current carrying wire. But in the case of a malfunction where current cannot pass through wire 4 because of a break, wire 4's resistance would go to infinity relative to wire 2's for example and the current would break through the reverse bias diode and flow around damaged cell B and back into wire 4.

The key to the annealing capabilities of the InP/GaSb solar cells is the operating temperature. For complete annealing of radiation damage, the InP material operating temperature must be above 100°C. In order to ensure this the Inp cells are wired with a forward bias configuration. This is shown in figure 4-6, where cells A, B, and C are wired with a forward bias configuration. After power is collected by the string of cells and passed along wire a small portion of the current is bled off and fed back through the cells themselves. The current can be divided by creating a 99:1 resistance ratio where 99% of the current would run through the wire with a relative resistance of 1, and 1% of the current would run through the wire with a relative resistance of 99. One percent of the total power should be enough to ensure that the operating temperature of the cells would remain above the 100°C mark. InP, being a semiconductor has a high resistivity and by a process similar to that of a light bulb filament the InP becomes heated when the current passes through it. It is assumed that the GaSb portion of the cell will receive negligible radiation damage due to the Kapton and silicon dioxide coatings behind it and the InP above.

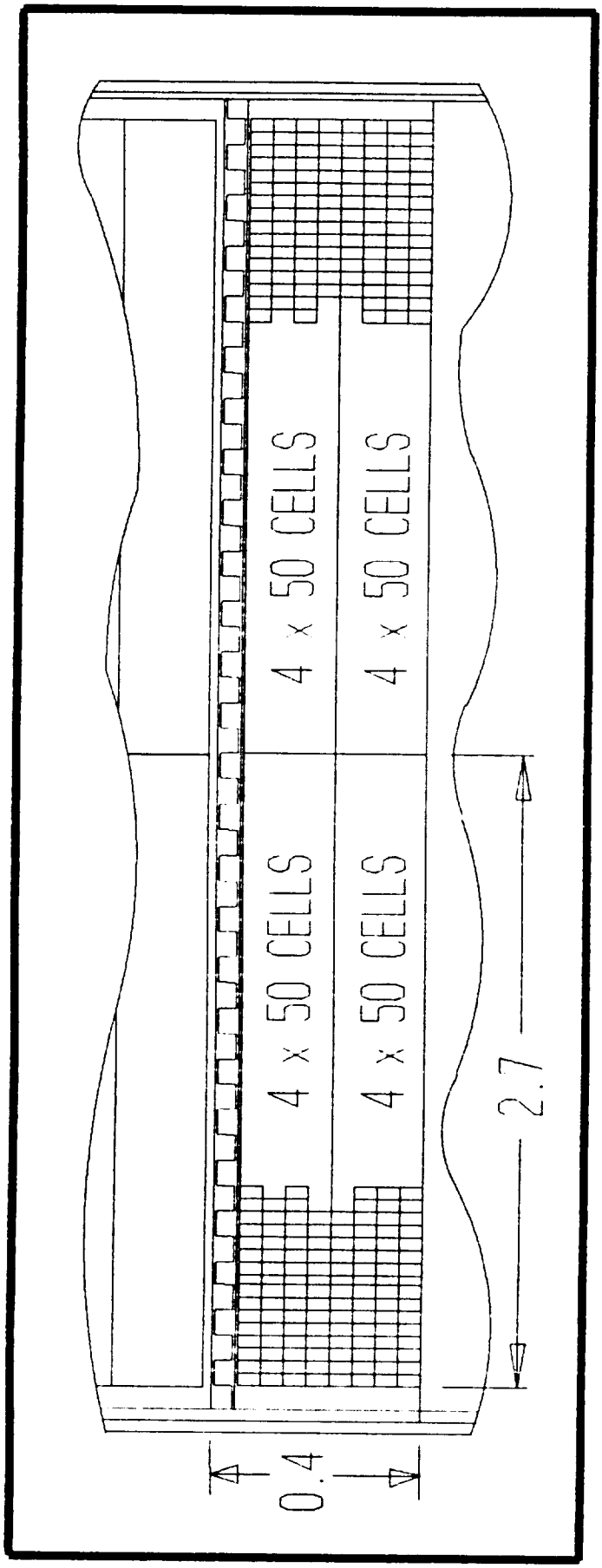

FIGURE 4-5

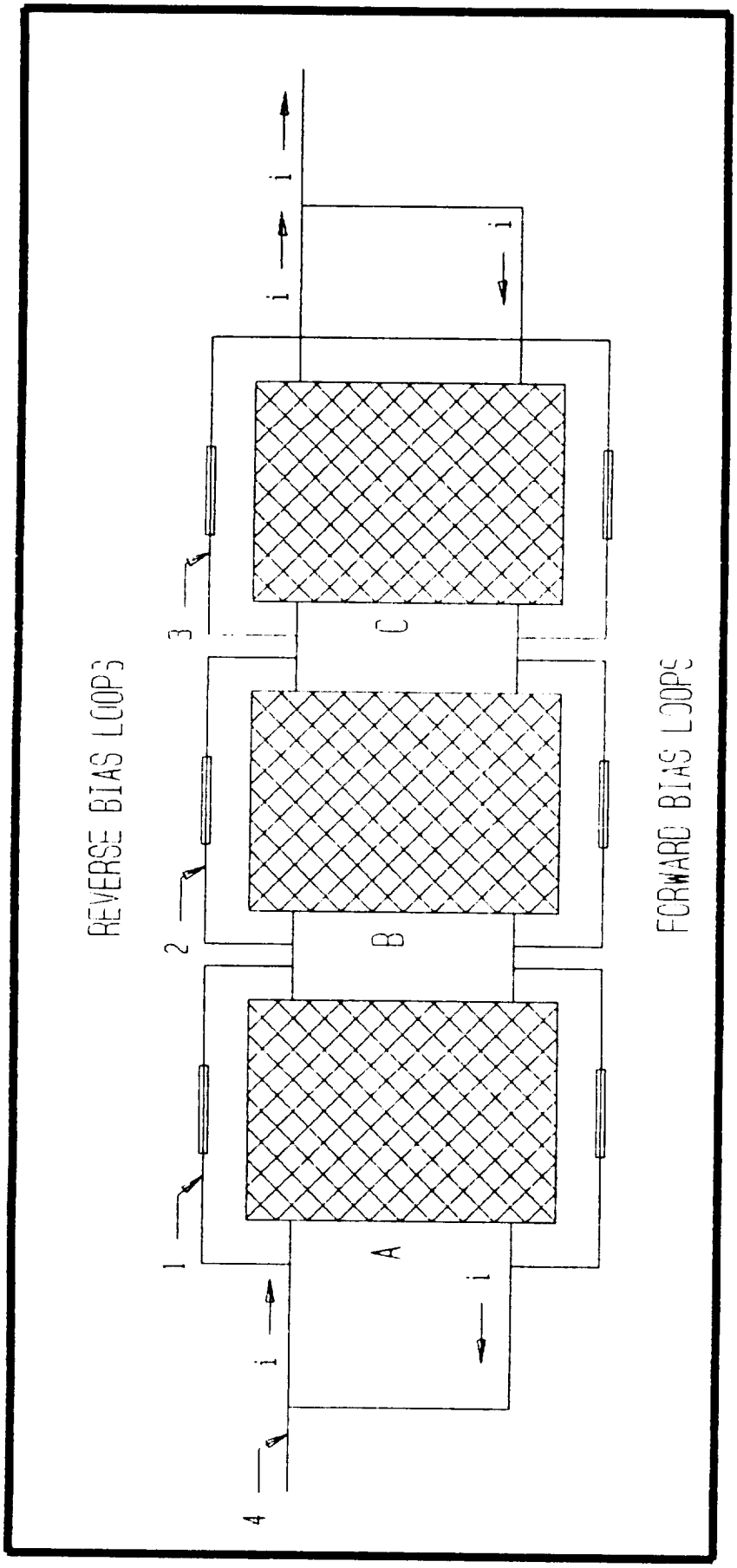

FIGURE 4-6

Each half array contains a total of 400 strings. These strings are added together in parallel giving each whole array an output of 1010.4 A at a voltage of 142.8 V. They are added in parallel to keep the voltage below the design limit of 200 V to avoid arcing between the solar cells. The total power provided from the twenty four individual deployable arrays is 24249.6 A at 142.8 V whose product yields a power of 3.463 MW, not discounting for degradation, resistive heating, wiring mismatches, etc.

All wires on the arrays are made of aluminum. Aluminum wires have a lower mass and a larger surface area than copper wires. This additional surface area allows the aluminum wires to radiate heat more efficiently than copper wires. In order to maintain an optimum level of electrical efficiency the wires must be kept cool whenever possible. Therefore the wires are attached and run along the shadow side of the solar arrays. The heavy wiring along the trusses is sized so that the power loss will be less than 80 kW.

4.3 Power Distribution and Management

Before the power from the arrays can be used it must first be conditioned into a form which can be used by the on-board systems and the thrusters. The current is run through a DC-AC converter then through a high frequency single phase transformer and power rectifiers. The power is distributed to on-board systems by the Power Distribution and Control Assemblies (PDCA). The essential part of the system constitutes power processing units (PPU) supplying power to ion thrusters (see section 3.3). The PDCA's are controlled by electrical power system software. The power system configuration is shown in figure 4-7(29).

SEMM1 is equipped with an auxiliary power system made up of two Nickel Hydrogen (NiH2) batteries packs. This system needs to run the ship when the solar arrays are in the shadow of the Earth (or Mars) and are not producing any power. The maximum shadow period, calculated from the trajectory of the ship, lasts around six hours. NiH2 batteries can produce up to 100 Watt-hours per kilogram(18). This makes them obviously too heavy to consider powering the main thrusters during shadow periods, so they are only used for housekeeping purposes like running the computers, communications, attitude control systems, and thruster starting controls. The battery system on SEMM1 can deliver up to 2 kW of power for nine hours. They are recharged continuously by extra power from the solar arrays. Two separate battery packs are used as a physical safety factor in the case that one of them may fail.

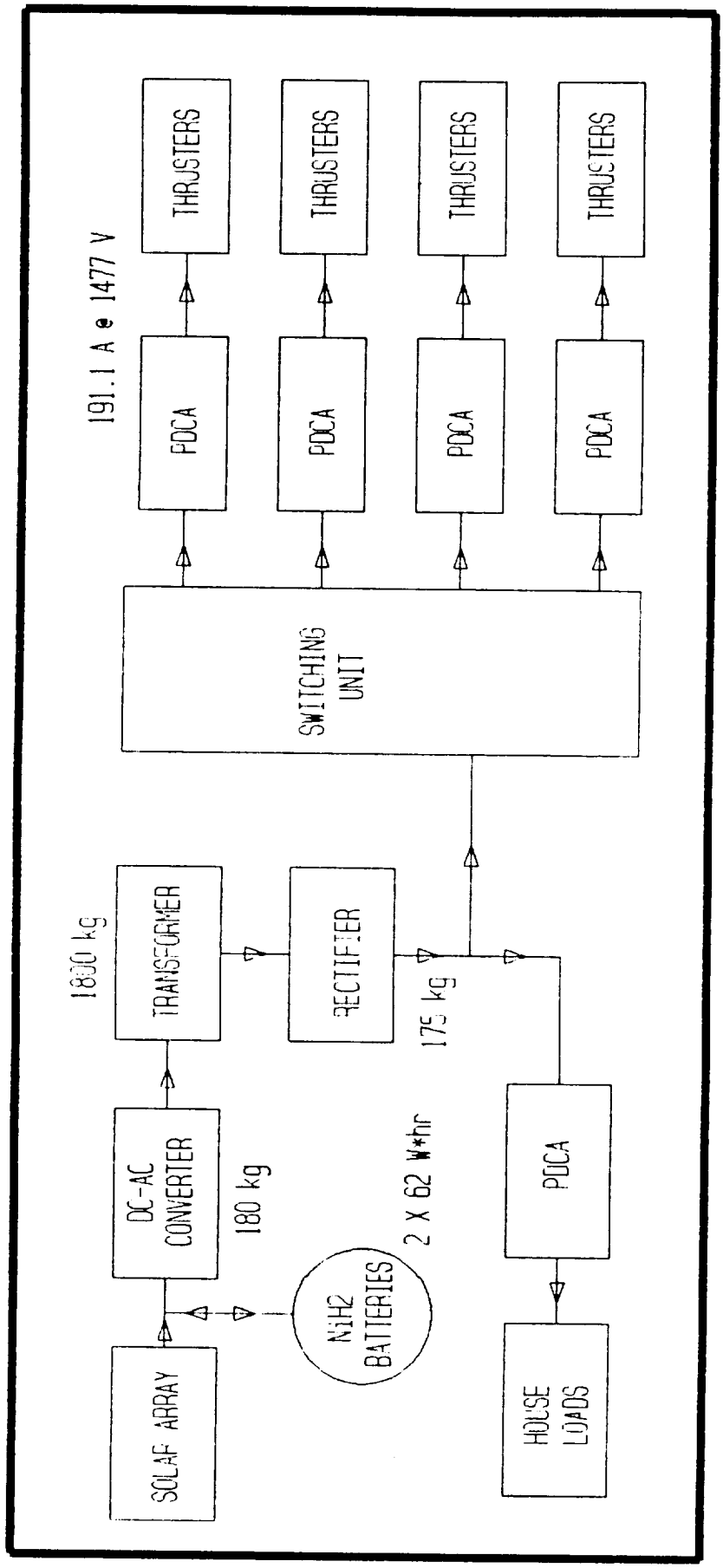
SOLAR ARRAY
DC-AC CONVERTER
180 kg
TRANSFORMER
1800 kg
RECTIFIER
175 kg
NiH2 BATTERIES
2 X 62 W*hr
PDCA
HOUSE LOADS
191.1 A @ 1477 V
SWITCHING UNIT
PDCA
PDCA
PDCA
PDCA
THRUSTERS
THRUSTERS
THRUSTERS
THRUSTERS

FIGURE 4-7

5. VEHICLE STRUCTURES

5.1 Truss Evolution

The initial configuration of the cargo ferry were based on using the mini-domed Fresnel lens system as stated in the Introduction. However, the problems involved with the supporting structure of the Fresnel lens array were judged as very difficult and serious. First, the accuracy of the array pointing must have been $\pm 1°$. This would be difficult to achieve without a very rigid panel, not to mention a possibly wobbly array. The system would have to be assembled on the large structure in space. Such an assembly would have required many hours of astronaut labor, and would have been very costly.

The next design step was to adopt the flat panels as the method of choice. When it was realized that the individual flexible blanket arrays could be mounted to a space station-like truss, efforts turned toward choosing the proper materials, strengths, and beam dimensions. Starting with graphite/epoxy, as the basic truss material, calculations quickly showed that the truss structure was inherently very strong. Large forces could be applied tc the beam with a very small deflection at the end. The next approach was to try to reduce the beam weight by using thinner and lighter rods, but it was found that the beam mass and strength remained relatively constant.

An important question at this point was how to shape the truss. One long truss beam seemed just as feasible as an H-shaped configuration, these configurations can be seen in figure 5-1. The comparison favored the long single beam, since simplicity is the key to easy assembly. The single beam created a greater moment on the alpha joints, but it reduced the moment of inertia of the wings, making them much easier to rotate.

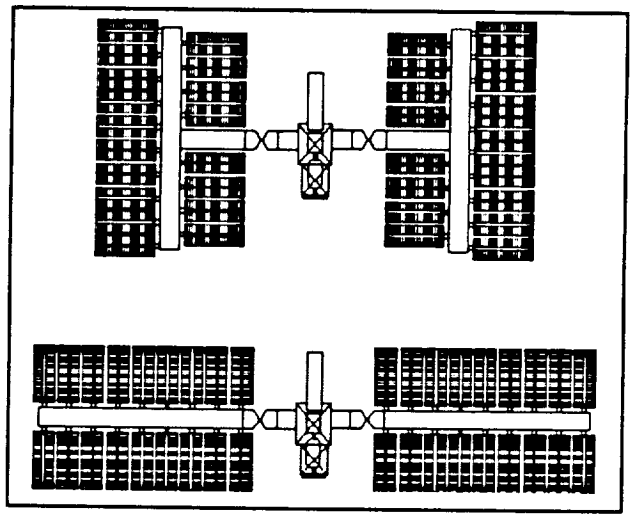

FIGURE 5-1

Focus then turned to rough optimization of the launch packaging capabilities. We assumed that a heavy lift vehicle (HLV) with an 8 meter diameter by 30 meter long cargo hold would be available at the time of our assembly. It was decided to launch the beam in preassembled sections to cut down on costly EVA time. This decision became a limiting factor in the beam dimensions. As seen in figure 5-2, four beam sections with 2.6 meter long sides will just fit into the HLV cargo bay. The arrays were placed in the bay, unattached, but alongside the truss, to be attached to the beam once in space.

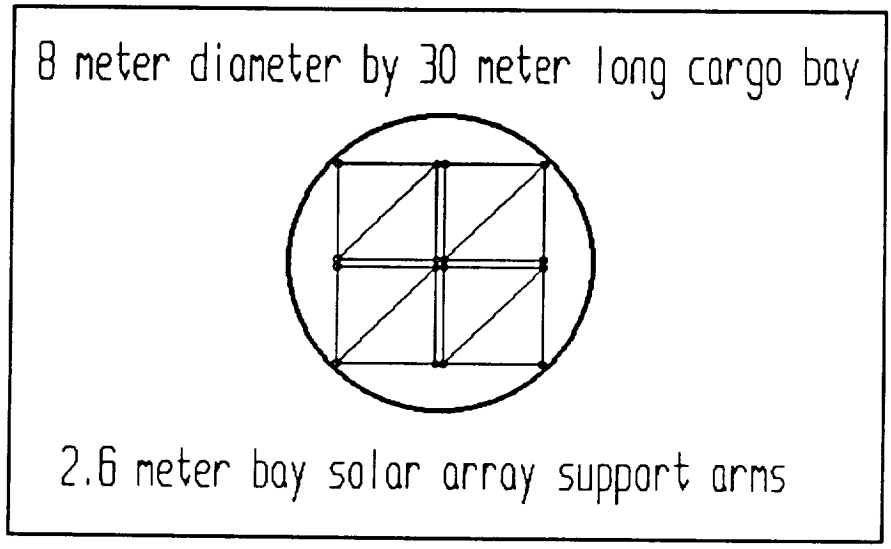

FIGURE 5-2

5.2 Materials Selection

The truss structure of SEMM 1 must be strong enough to support solar arrays about the size of a football without deflecting too much at the ends. The key component of modern space structure is a composite tube. A composite tube must not only strong, but must be able to withstand thermal cycling as well as deterioration due to radiation and atomic oxygen.

Thermal cycling in LEO typically is between 150 and -100 degrees Fahrenheit. This presents a problem for some composite materials because they develop microcracks when thermally cycled. A suitable composite for our needs must have a low coefficient of thermal expansion (CTE), to minimize dimensional changes through the temperature cycle. Table 5-1 shows the modulus of elasticity and the CTE for several composites. Also included is an assessment of radiation resistance.

Material	E ($psix10^6$)	CTE($in/in/Fx10^6$)	Radiation Resistance
Gr/Epoxy	39	-0.6* / 18**	good
Gr/Glass	31	-0.3* / 3.6**	good
Gr/Al	47	0.8* / 15**	-
Aluminum	10	13	-
Titanium	17	5	-
Gr/Mg	high	-0.04 to 0.16**	Excellent
* Longitudinal ** Transverse			

TABLE 5-1 COMPOSITE MATERIALS COMPARISON

Gr/Mg seems to be the overall best candidate for space structures, but it has one major problem. If it is cycled to temperatures reaching $-200^{\circ}F$ it will experience cracking and possible fracture. The choice then becomes difficult because Gr/Al and Gr/Epoxy are statistically very similar. Gr/Al has a higher modulus of elasticity, but Gr/Epoxy has a higher ultimate axial tensile strength of 1.34×10^9 N/m^2 than titanium which has an ultimate tensile strength of 1.10×10^9 N/m^2. Gr/Epoxy also has good resistance to radiation.

The possibility of using a coating to protect the structure from UV radiation and atomic oxygen exists. A thin coating of reflective Aluminum on the composite tubes would improve radiation protection and keep down the temperature of the structure when exposed to the sun.

Gr/Epoxy tubes combined with titanium nodes seem to be a good combination because they have similar CTE's. This means that they will contract and expand similarly thus reducing stress and strain on the joints where they are bonded together. Titanium nodes were chosen purely for their higher strength than that of aluminum.

5.3 Truss Element Calculations

The power structure truss reaches out 72.8 meters past the alpha joints, and is built of hollow composite struts, attached by multijointed nodes in a boxlike beam, as seen in figure 5-3. The truss is strong enough that even at extreme inertial loads, such as those created on impact with a Space Station, the tip of the truss will bend less than 0.5 meters. The truss will be launched in six fully assembled sections, to be connected in LEO.

The truss elements will be made of graphite/epoxy and will be connected by titanium joints. The truss elements will be hollow with a 3 cm outer diameter and a 1.5 mm wall thickness, as seen in figure 5-4. Each element will be protected with a 0.1 mm coating of anodized Aluminum. The calculations for the truss element dimensions are presented in Appendix C. The density of graphite/epoxy is 1522 kg/m^3, and the density of titanium is 4510 kg/m^3. There will be 28 box bays per arm, so there will be 228 truss elements 2.6 meter long (0.53 kg each), 141 truss elements of 3.7 meter long (0.76 kg each), 116 node joints (1 kg each), and 12 interface components (9 kg each) where the panel modules attach.

Mass Summary:

2.6 m elements	121 kg
3.7 m elements	106 kg
node joints	116 kg
interface components	108 kg
total truss arm	451 kg

This arm weight does not include electrical wiring or the weight of the alpha joints.

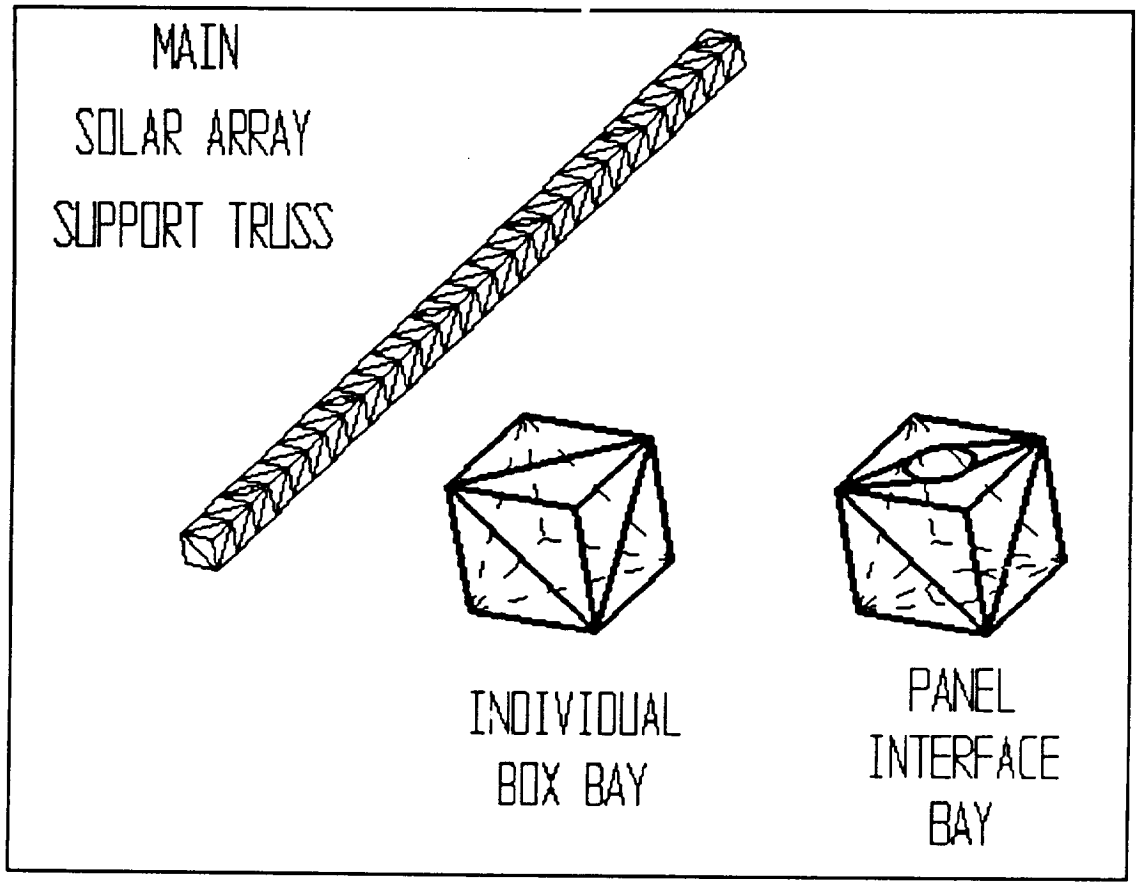

FIGURE 5-3

Mass summary of the solar power system is given in Table 5-2.

24 Solar Arrays	12,120 kg
Wiring	1,400 kg
Trusses, α-rotational joints with sliding electrical connectors	1,800 kg
Total Mass	15,320 kg

TABLE 5-2 POWER SYSTEM MASS SUMMARY

5.4 SHIELDING

Outer space has some serious environmental problems. These include space debris, micrometeorides, atomic oxygen, thermal cycling, charged particles and ultraviolet radiation. Space debris held in orbit about the earth have very high velocities. The cargo vehicle will have to travel through regions where there will be a high probability of impact by micrometeoroids and space debris, so shielding must be provided for the ship's vital systems. The fuel tank, the navigation/communication systems and the cargo module will need to be protected. The tank shielding is discussed in Section 3.1. The shielding will consist of a series of corrugations backed by two bumper plates spaced away from the spacecraft wall, as seen in figure 5-4. The corrugation will enhance the protection and help prevent the creation of ricochet debris(42) which could strike other parts of the spacecraft. The large solar arrays cannot be shielded from space debris, so we have allowed for degradation due to debris collisions by making the solar arrays about 2% larger than necessary, and this will also serve to account for degradation due to solar radiation. To reduce degradation caused by thermal cycling, abrasion and exposure to atomic oxygen, the structural parts of the craft will be protected by coating with anodized Aluminum.

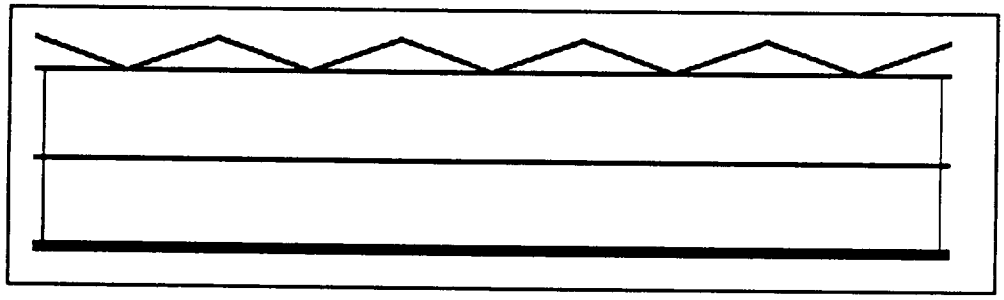

FIGURE 5-4

6. GNC & COMMUNICATIONS SYSTEMS

A Guidance, Navigation and Control system and a Communications System are vital to the success of the mission. The communications system provides data and image transmissions to Earth so that the mission can be monitored and controlled. Corrections and adjustments that need to be made are then transmitted back to the spacecraft. Any maneuvers that need to be made are then performed.

6.1 COMMUNICATIONS

In designing a communication system several factors must be examined. The first critical option is the amount of information that must be transmitted. Second is the amount of time available to the craft for the actual transmitting of the data. Lastly, the distance over which the data must be sent. With the maximum data rate set at 20 Mbps, the decision became a trade-off between antenna size and broadcast power(39).

To support our communication system, several assumptions were made as to the technological developments that will occur by the launch of the spacecraft. First, NASA's Deep Space Network (DSN) will be upgraded to a quad 34 m Ka-band system giving an effective aperture of 70 m. Secondly, there will be two Mars Relay Satellites (MRS) in a stationary orbit 120° apart. Lastly, there will be some distributed Mars Surface Terminals (MST).

Analysis of the return links was emphasized due to the fact that uplinks from the Earth were far less critical. Building large antennae and acquiring the power needed to operate is far easier to accomplish on Earth than in deep space.

The communications system is composed of the two MRS, DSN, the MST and the cargo ferry. The MRS provide all intrasystem communications and the major communication links with Earth. The advantages of this system, as opposed to one with less or no MRS, is that there is near 100% coverage and provides full connectivity. The communications system operates at Ka-band (32.05 GHz).

The spacecraft itself will carry four antennae: two fully directional parabolic reflector antennae and two spiked-horn omni-directional antennae. The parabolic reflectors are 5 m in diameter and the omni-directioanl antennae have a length of 0.5 m(39). The antennae are made of a graphite-fiber-epoxy (GFE). The parabolic reflectors are used for the majority of the communications needs. The omni-directional antennae are used at close ranges, such as for communications with MRS while in orbit at Mars and docking maneuvers.

The MRS to DSN is the most critical link. A data rate of 10 Mbps is achieved using a 9 m MRS antenna. This requires 180 W of power. Crosslinks between the MRS can reach data rates of 40 Mbps with antennae diameters of 1 m and 2.3 W of power. For direct links between the spacecraft and DSN, the 5 m parabolic reflector

requires 182 W of power and can transmit 10 Mbps. For links between the spacecraft and MRS, the 0.5 m long omni-directional antenna is used. This requires only 6.6 W of power.(39) These links are summarized by figure 6-1 and table 6-1. The mass and power of the components of the system are given in table 6-2.

The command subsystem is responsible for uplinks to the spacecraft. Relay commands and data commands are the two basic command types.

Relay commands may be simple on/off type functions or initiate a step-by-step procedure. Data commands give information upon which the spacecraft acts. For example, firing a thruster to correct the actual trajectory would be a combination of relay and data commands. Data commands might include instructions for orientation of the craft and time to burn. The relay commands could be switching from one antenna to another. This also illustrates the need for delayed commands. If the burn needed to be planned ahead of time, it would not be wise to wait until just before the burn is to occur to transmit the command. So, transmitting the whole sequence of events ahead of time is necessary.

The commands are received by the antenna and sent to the receiver. The receiver amplifies the signal and filters it to achieve a "cleaner" signal and to get rid of unwanted signals and noise. The command then goes to the command processor where it is interpreted. The simple commands then go straight to the power switching unit and are executed. Delayed commands are stored for action at a later time. More intricate commands are sent to the computer to be sorted out before execution. This command subsystem is depicted in figure 6-2.

The telemetry subsystem (figure 6-3) is the opposite of the command system, so to speak. Where the command system dealt with receiving signals, the telemetry subsystem deals with transmitting data. Sensors respond to some event, such as an acceleration, and send it to be converted into an acceptable form for transmission. Weak signals are amplified and strong signals are attenuated. If transmission is possible the signal is sent. Otherwise, the data is stored and transmitted at a later time.

DATA LINK	FREQUENCY (GHz)	TRANSMIT POWER (W)	TRANSMIT ANTENNA DIAMETER (m)	RECEIVER ANTENNA DIAMETER (m)	DATA RATE (Mbps)
MRS TO MRS	32.05	2.3	1.0	1.0	40.0
MRS TO GT	32.05	180.0	9.0	70.0	10.0
SEMMI TO MRS	32.05	8.6	0.5	1.0	20.0
SEMMI TO GT	32.05	182.0	5.0	70.0	3.8
MST TO MRS	32.05	5.7	0.5	1.0	50.0

TABLE 6-1

	QUANTITY	MASS (kg)	POWER (W)	SIZE
COMPUTER MSSC-II	2	8.0	240.0	6 LITERS
PARABOLIC REFLECTOR	2	20.0	182.0	5 m DIAM
OMNI-DIRECTIONAL ANTENNA	2	1.0	6.6	0.5 m DIAM
CMG	4	190.0	40.0	0.25 m DIAM x 0.25 m LENGTH
RIG	4	0.77	16.0	0.06 m DIAM x 0.28 m LENGTH
FREON GAS JET	20	0.5	20.0	0.3 m DIAM x 0.5 m LENGTH

TABLE 6-2

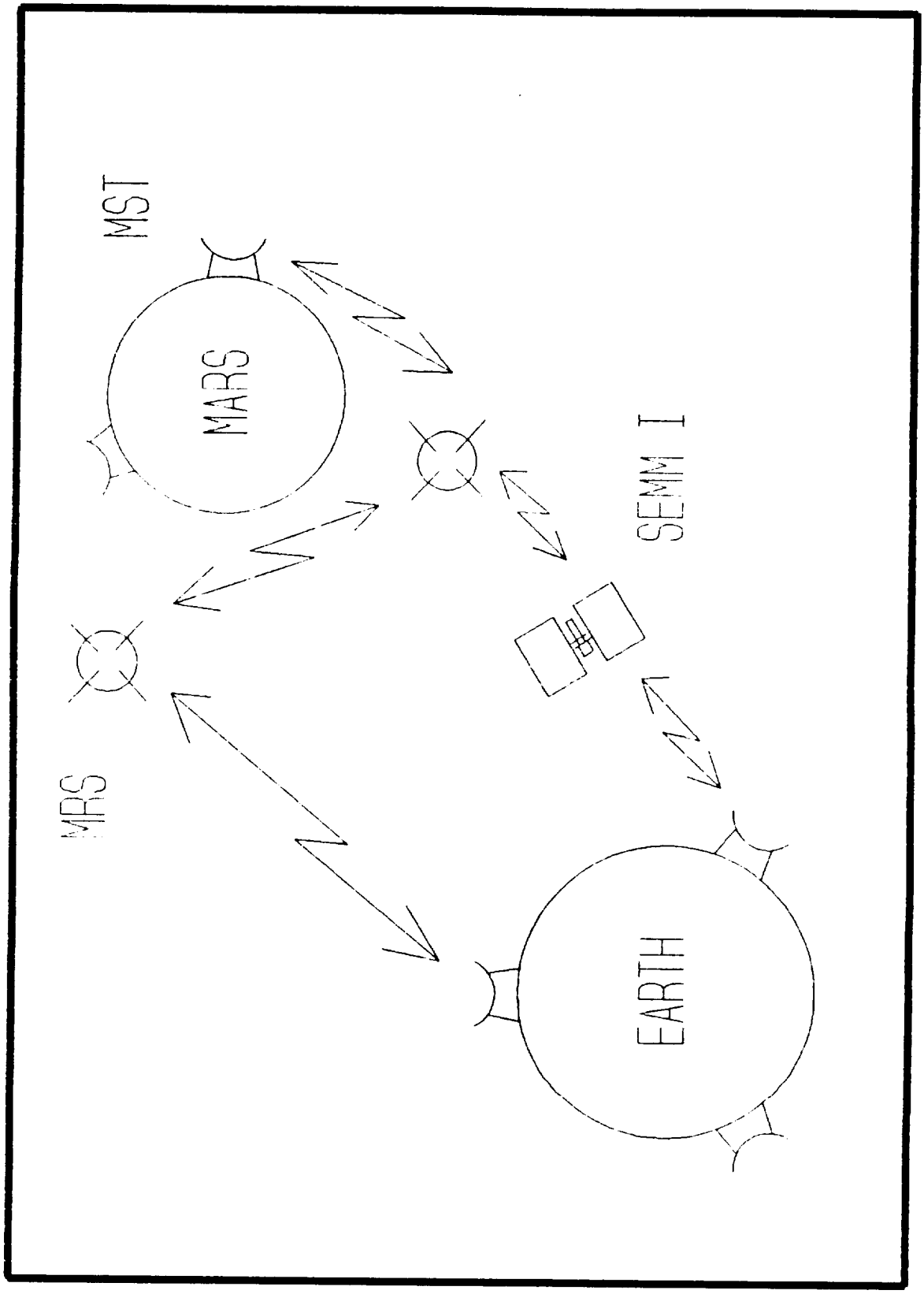

FIGURE 6-1

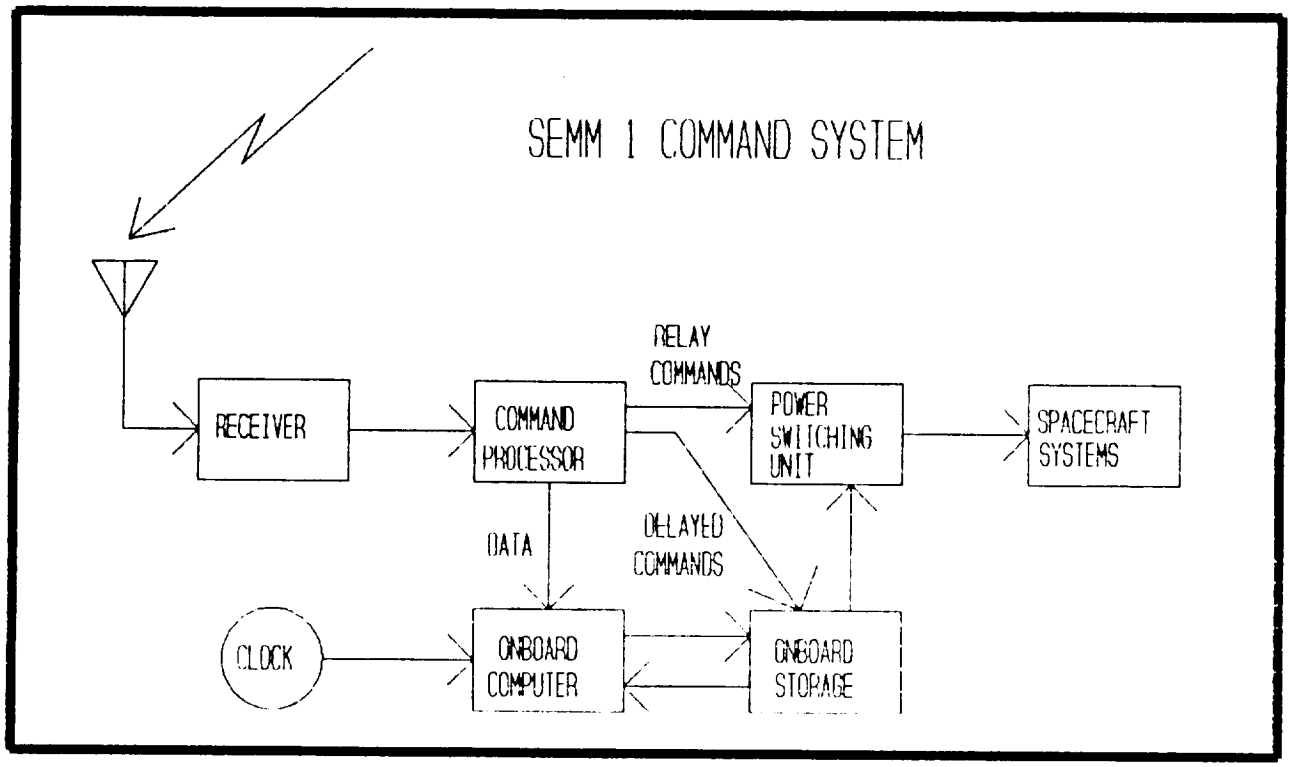

FIGURE 6-2

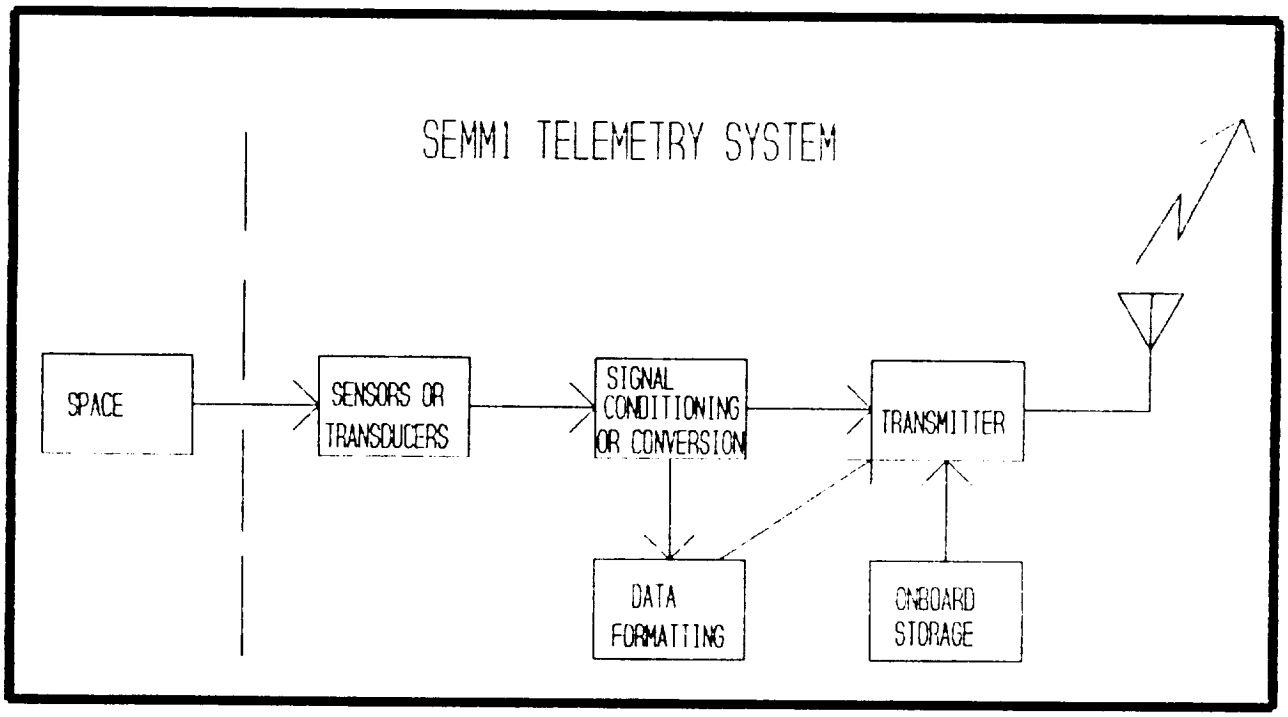

FIGURE 6-3

6.2 Guidance, Navigation, Control

The cargo ferry requires a command management system that can bring it to Mars. The guidance, navigation, and control systems are necessary to keep the ship on course. Another important function is to keep the solar arrays facing the sun. Well before the craft is launched, the planned trajectories as well as alternate routes and contingency plans are fed into the computer by engineers. The ship's computers handle all functions on the ship, but draw less than one kilowatt of power. There are two computers for every function, since electrical failures can be expected to occur.

Once launched from Space Station Freedom, SEMM1 must receive data from various sensors, such as star trackers, that fix the ship's position in space. Information on location and attitude must be compared to the model trajectory stored in memory. A feedback control law issues commands to the ship's control system to correct errors in flight path.

The ship's navigation system uses a system of Inertial Measurement Units (IMU), scanning telescope, spacecraft transponders and a guidance and navigation computer.

Sun sensors on the solar arrays are used to track the sun during the journey through space. There are four double-axis sun sensors on the upper surface of each truss beam. They are small boxes, illustrated in figure 6-4, no more than 1 kg in weight and are mounted at the end of each arm. These sensors use square apertures above photocells to detect changes in the direction of incident sunlight (53). This information is fed into the computers which relay commands to the control moment gyroscopes (CMG) to slowly turn the solar arrays. The accuracy of the sun sensors is much more precise than the arrays actually need due to their pointing tolerance.

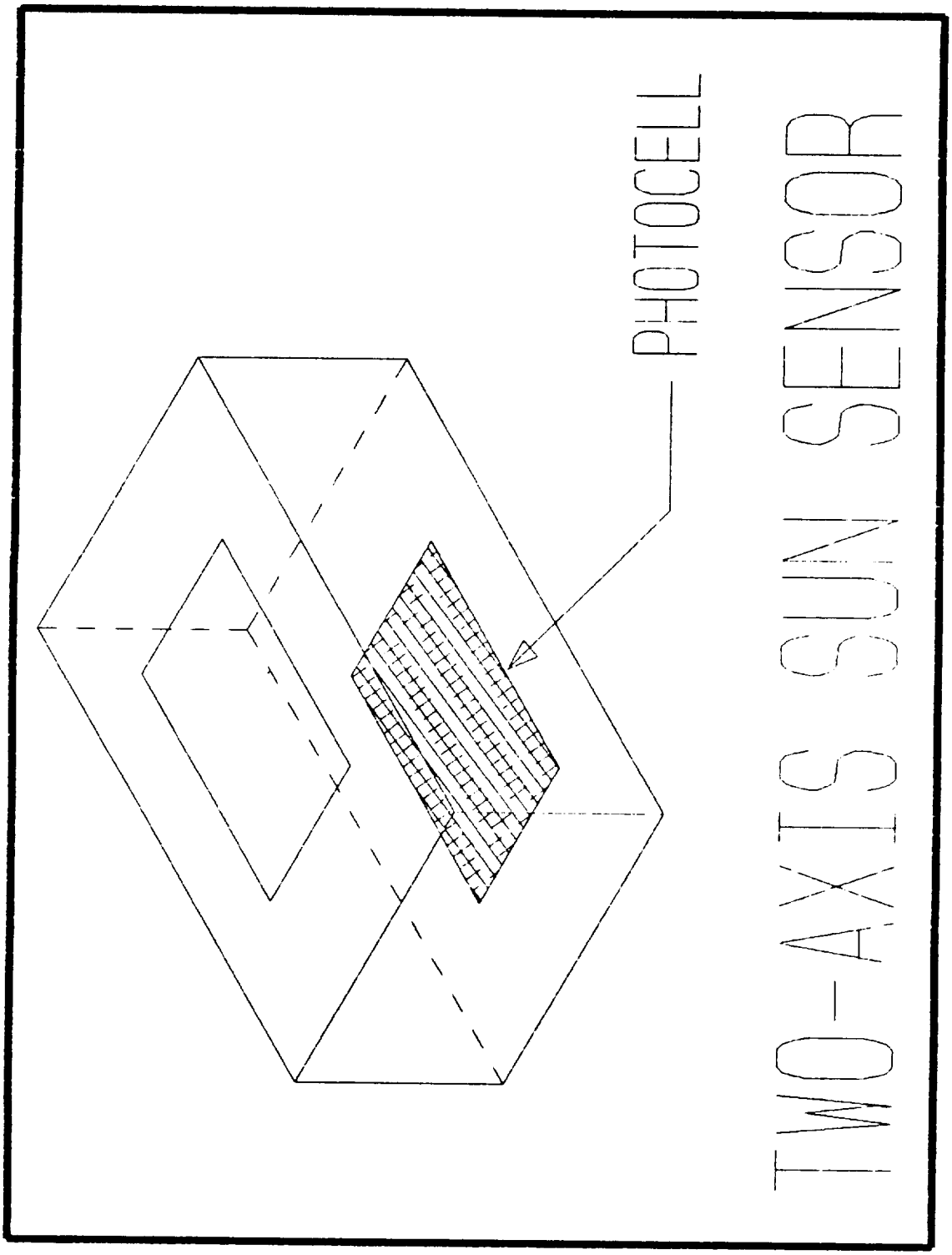

FIGURE 6-4

The ship must have controls that determine pitch, yaw, and roll, where the x-axis is assumed to pass from the cargo to the thrusters. The acceleration vector of the ship will most always be along this axis under thrusting conditions. Small corrections will be made by the control system, made up of a trio of control moment gyros and several small thrusters mounted on the structure.

The control moment gyros (CMG) provide the primary rotational control for the vehicle. This motion produces a powerful pure moment vector that in essence is fixed in space. Any perturbations to this vector will result in a restoring motion that will keep the vector pointed in its original direction. This can be used by the ship to control its attitude. Electrical motors are used to turn the gyro's mountings, disturbing its direction. When the gyro torque corrects its orientation, the entire ship is forced to rotate opposite to this motion.

SEMM1 will use four such gyros, housed in the central body module. They produce a pure couple that will rotate the ship independent of its location. Three gyros will point in each of the three coordinate axes, while the fourth serves as redundancy. A gyro currently made by Bendix is recommended as the baseline standard, though improvements in technology may well provide a significantly improved gyro. The example is detailed as follows:

Weight:	190 kg
Rotor Speed:	4,000 rpm
Maximum Output Torque:	250 Nm
Gimbal Freedom (deg):	unlimited
Approximate Size:	cylinder 1.25 m diameter X .50 m long

TABLE 6-3

Very slow rotations about y (array truss direction) and z-axis, required during main thrusting for midcourse corrections, can be accomplished by differential thrust and/or gimballing of the main thrusters.

The secondary control system is designed for rotations about x (roll) and y-axis and for small translational adjustments. The system can be provided by small ion argon thrusters mounted at the corners of the main body structure. These thrusters would use the same power source and propellant tank as the main thrusters. Such a system provides a virtually unlimited attitude control capability. Alternatively, a cold gas system may be applied. The cold gas system operates more consistently than a hot gas jet, particularly when the system is operated in a pulsed mode, because there is no chemical reaction which must reach steady state. The low thrust level therefore facilitates more precise control(53). This system is only necessary in the docking maneuvers required at Mars and with Freedom and/or for desaturization of CMG's. Each gas thruster includes its own small fuel tank of freon propellant,

and produces one newton of thrust while thrusting. The jet is only 0.5 meter long with a nozzle diameter of 0.3 meter.

Twenty-four jets will be mounted on the corners of the body module, three on each corner, one pointing in each direction. Each face therefore has four jets that will provide 4 N of thrust perpendicular to that face. Combinations of firings can provide translational motion in any direction. The gas system has multiple redundancy, since up to three jets can fail on any face. The jets also serve as a redundancy for the CMG attitude control and a last ditch source of power in case of an unlikely ion thruster shutdown.

Both systems respond to commands from the central control system found in the main body housing. This system monitors the ship's position and uses an error feedback loop to make corrections.

7.0 VEHICLE LAUNCH AND MAINTENANCE

The Mars cargo ferry must begin its mission from LEO. However, the machinery and components are built and tested on Earth. The task of getting the ship into orbit and assembled is a very practical and very important consideration.

7.1 Launch Packaging

By the year 2005, an HLV will be in operation. The boosting of all the pieces into LEO will require three full size launches. The launch scheme is illustrated in Figure 7-1. The HLV will bring the pre-assembled pieces to the Space Station Freedom, where the robots and astronauts will receive the cargo. SEMM1 is built in modules that can be easily removed from the cargo bay of the HLV and attached to one another with a minimum amount of construction time. The launch schedule is below:

Launch 1:	16 solar arrays, four 28.6 m truss sections
Launch 2:	main body module, thruster module, 2 alpha joints, 8 solar arrays, four 7.8 m truss sections,
Launch 3:	cargo

The first launch will contain a portion of the pre-fabricated truss beam and several of the photovoltaic power modules. The HLV cargo bay is assumed to be cylindrical, 7 meters in diameter and 30 meters long. The 2.6 meter truss bays enable four separate lengths of the beam to be stacked in the cargo bay. The power modules will be stored in the space between the beams and the wall of the HLV. Upon reaching Space Station Freedom, the truss section will be removed by the station's remote manipulator arm. The arm will bring the section inside an assembly area on the station's upper boom. This construction bay is much like an airplane hangar, open at both ends. The sections will be attached to the frame and held until the assembly begins.

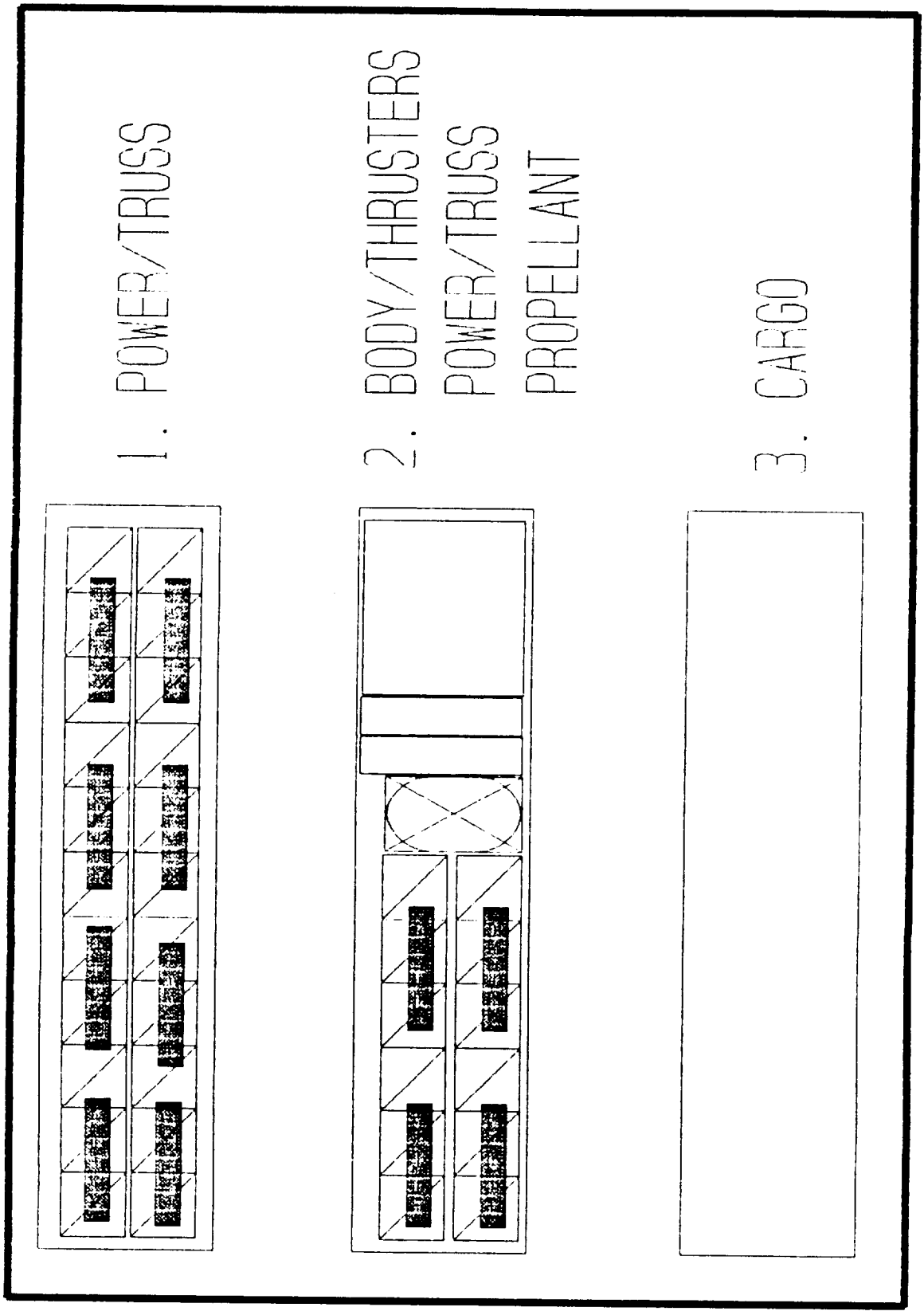
1. POWER/TRUSS
2. BODY/THRUSTERS
POWER/TRUSS
PROPELLANT
3. CARGO

FIGURE 7-1

7.2 Assembly

Actual assembly of the pieces, if conducted in early 2000, will most likely use space-suited astronauts who will manually bring the sections together, as shown in Figure 7-2, joining the final struts and nodes. This EVA method of construction would be very costly, time consuming and subject to hazards.

By 2010 telerobotic methods of construction combining the durability of a robotic manipulator and the intellect of a human operator may become available. The man will operate the robot arms from the safety of a crew workstation, using joysticks or electrically wired gloves that relay the man's movements directly to the robot's manipulators. Telerobotics may be ideal for construction of SEMM1 since the final assembly will be simply a matter of attaching one node to a strut, something the robotic arms could handle easily.

The two solar array support arms are each over 70 meters in length, so upon completion they must be attached side by side to the exterior truss of the space station, above the upper keel. The truss is so light that its presence will not adversely affect the performance of the station, nor will its thin members block sunlight to Space Station Freedom's arrays.

The second launch will contain the main body module, the thruster module, the alpha joints, the propellant tank, and additional power modules. Except for the truss and arrays. Once the tank is installed on the body, the solar array support arms will be carefully fixed into the sides to complete the assembly. The final SEMM1 assembly must take place on the upper boom of the space station, as the pieces are simply too large to fit in the garage. The ship will remain completed on the upper boom until the cargo arrives for the trip to Mars.

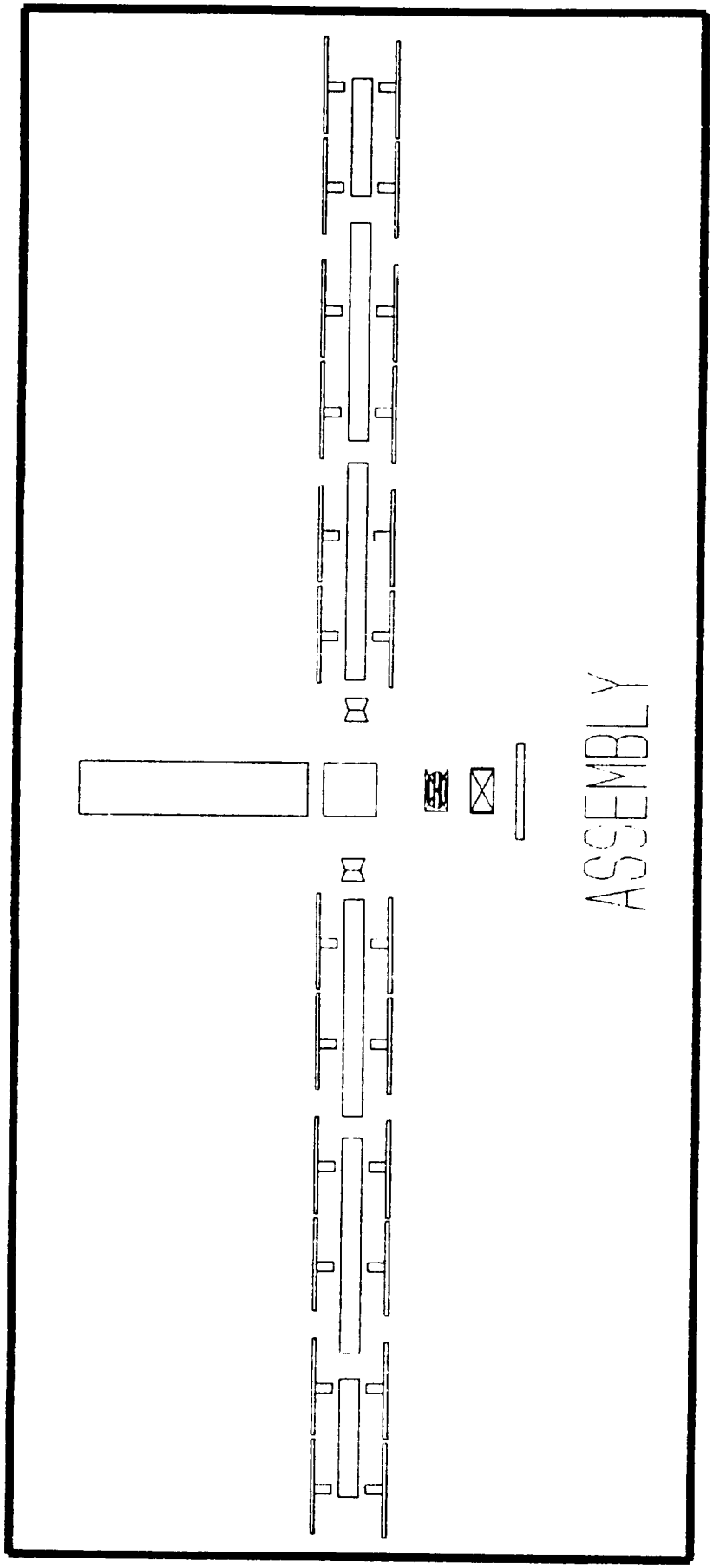

FIGURE 7-2

7.3 Docking

The cargo ship is built for one reason; to move material to Mars orbit. To accomplish the mission an ability to dock with a servicing vessel in orbit around Mars, and then again with the Space Station Freedom on the return trip to Earth may, perhaps, be required. Docking would be the most strenuous activity the ship may encounter. The huge ferry, weighing 120,000 kg, must be brought to a complete and sudden stop. Considering the ferry's approach speed at 1-2 cm/sec, and a deceleration lasting one-tenth of a second, the forces on impact with Freedom will cause an inertial force of nearly 20 N on each solar array. The truss structure was designed to withstand this stress easily. In addition, the docking mechanisms of both crafts have attenuation devices that cushion or absorb some of the momentum of the impact.

Realistically, though, there are problems associated with docking at Freedom on the return trip. The ferry is over 150 meters long, which is as large as the Space Station itself. The presence of the huge cargo ship could get in the way of other station functions and might block the sun from the station's own solar panels. In addition, the station doubles as an Earth observation platform, and any blockage of view from the bottom of Freedom will not be allowed. Fortunately, there is no transfer of crew that would need an airlock connection. All the inspections and maintenance that might need to be performed on the ferry will be carried out by robotic surveillance or space-suited astronauts.

The cargo vessel, therefore, will not dock at the usual shuttle pressurized berthing nodes. SEMM1 will approach the station and match its speed and orbit very closely. Freedom flies at an inclination of 28.5° at an altitude of 250 nautical miles. The station's attitude with the Earth remains constant, meaning there is a constant "top" and "bottom" to the structure. Using small adjustments with its gas jet maneuver system, the craft will drift close to the station and remain there until it is launched again for Mars.

Most likely, docking with a Mars orbiting station will not be required. Once the cargo ship enters the prescribed Low Mars Orbit, the payload may be released by means of very small solid rockets.

7.4 Maintenance

The ferry will remain close by for several months while all systems are checked out by free-flying robotic surveillance equipment. These miniature satellites can scan and detect any crack, stress, or deformation to the structure and arrays. In addition, the computers will be run through a full diagnostic routine before implantation of new commands and trajectories begins.

The ship is designed to last for three journeys to Mars and back. This will go on over a lifetime of twelve or more years. The solar arrays should not need replacement unless a cataclysmic collision has occurred. The truss should last at least fifteen years, especially with the protective anti-deterioration coating. Defective ion thrusters can be changed out either by the servicing satellites using telerobotic control (preferred) or a space-walking astronaut. Malfunctioning interior equipment will be harder to replace, so a hatch has been installed that will allow an astronaut access to the electrical components.

8.0 DESIGN SUMMARY

The cargo ferry outlined in this paper was designed to bring a load of machinery or materials to Mars. The ship uses photovoltaic solar cells to power ion thrusters and follows a trajectory of spirals; first out from Earth, then around the sun, finally spiralling down to low Mars orbit.

The spacecraft mass summary and the main specifications are shown in Tables 8-1 and 8-2 respectively.

	kg
Cargo	61,000
Cargo Housing/Protection	2,000
Argon Propellant	23,840
Tank, Propellant Handling System	850
Propulsion System (including PPU)	9,750
Solar Panels	12,120
Solar Array Support Truss, α-Joints, Sliding Electrical Connectors	1,800
Wiring	1,400
Main Body Structure	1,200
Auxiliary Power (Batteries), PDSC	1,050
GMC, RCS	2,100
GNC/Communication System	800
Payload Release Equipment and/or Docking Mechanisms	400
TOTAL MASS	118,130 kg

Table 8-1 SPACECRAFT MASS SUMMARY

Cargo Mass	61,000 k
Cargo Volume	30 m X 7 m dia.
Cell Type	InP/GaSb
Specific Pwr.	303.6 W/m^2
Solar Array Area	10,368 m^2
Array Power	3.06 MWe
Isp (Argon)	8,000 seconds
Propellant Mass	23,840 kg
Tank Size	5.1 m x 2.55m(ellipsoid)
Thruster Size	2 m dia.
Number of Thrusters	13 (10 in use)
Thrust (LEO)	60 N
Trip to Mars	654 days
Time at Mars	14 days
Return Trip	479 days
HLV Launches	3
Total Mass (LEO)	118,130 kg
Payload Mass Ratio	0.516

Table 8-2 SPACECRAFT SPECIFICATIONS SUMMARY

Our study indicates that an SEP cargo ferry using high Isp thrusters and advanced planar solar arrays may offer significant advantages in terms of low initial mass and a high payload mass ratio. Realization of these advantages will depend on the progress in solar cell technology. It appears quite reasonable to expect, that during the next 12-18 years, cell conversion efficiency and resistance to radiation damage will reach levels assumed in this study.

APPENDIX A

Truss Element Dimension Calculations

In designing structures one uses the largest anticipated loads, for our case that would be docking. In deriving the loads we assumed docking with the Space Station Freedom, an approach speed of 2 cm/sec, and an impulse of 0.25 sec.

$$m_1 * V_1 = m_2 * V_2$$

$$135{,}000 * .02 = (135{,}000+500{,}000) * V_2$$

====> $V_2 = 0.004252$ m/sec

====> $$a = \frac{V_1 - V_2}{\Delta t} = \frac{.02-.004252}{0.25} = 0.0630 \text{ m/sec}_2$$

mass of solar panel modules = 490 kg

====> $F = m * a = 490 * 0.0630 = 31$ N

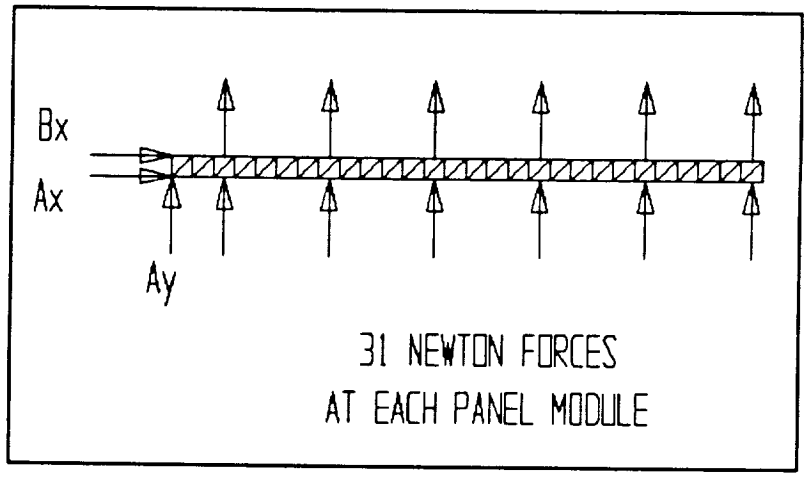

FIGURE A-1

Find element diameter for critical buckling.

$M_A = 62(6.5 + 19.5 + 32.5 + 45.5 + 58.5 + 71.5) - B_X(2.6) = 0$

$B_X = 5580$ $A_X = 5580$ $A_Y = 372$ $I = \frac{\pi}{4}(r_2^4 - r_1^4)$

$$P_{CR} = \frac{\pi^2 EI}{L_e^2} \qquad E = 2.689 * 10^{11}\ N/m^2$$

FIXED-PINNED

$L_e = 0.7(2.6\ m) = 1.82\ m$

$P_{CR} = F.S.* B_x = 1.5 * 5580$

$= 8370\ N$

$$\Longrightarrow I = \frac{P_{CR} L_e^2}{\pi^2 E} = \frac{\pi}{4}(r_2^4 - r_1^4)$$

$$\Longrightarrow (r_2^4 - r_1^4) = \frac{4 P_{CR} L_e^2}{\pi^3 E} = \frac{4\ (8370)\ (1.82)^2}{\pi^3\ (2.689 * 10^{11})}$$

$$(r_2^4 - r_1^4) = 1.33 * 10^{-8}\ m^4 = 1.330\ cm^4$$

for element thickness of 1.5 mm.

$\Longrightarrow r_2 = r_1 + .15$ cm

$\Longrightarrow r_2 = 1.40$ cm & $r_1 = 1.25$ cm

rounded up to nearest quarter cm for outer diameter

$\Longrightarrow d_2 = 3.00$ cm & $d_1 = 2.70$ cm

Calculation of critical stress

$A = \pi\ (r_2^2 - r_1^2) = 1.343 * 10^{-4}\ m^2$

$$\sigma_{CR} = \frac{P_{CR}}{A} = \frac{8370}{1.343 * 10^{-4}} = 6.232 * 10^7\ N/m^2 \times \frac{1\ psi}{6895\ N/m^2}$$

$\sigma_{CR} = 0.9039$ ksi << 24,000 ksi (strength of Graphite/Epoxy in compression)

Calculation of stress due to bending moment

$V = 1.343 * 10^{-4}\ m^2 \times [\ 224(2.6\ m) + 84(2.6\sqrt{2}\ m)\ ] = 0.1197\ m^3$

$A = V/L = 0.1197/72.8 = 1.644 * 10^{-3}\ m^2$

for a square where s = side length and c = s/2

====> $s = 0.0406\ m$ ====> $c = 0.0203\ m$

see figure 5.2-2 for moment calculation

$M = F.S.* B_x * 2.6 = 1.5 * 5580 * 2.6 = 21{,}762\ N\ m$

$$\sigma = \frac{M\ c}{I} = \frac{21762\ (0.0203)}{1/12\ \ (0.0406)^4} = 1.951 * 10^{10}\ N/m^2 \times \frac{1\ psi}{6895\ N/m^2}$$

$\sigma = 282\ ksi << 24{,}000\ ksi$

Calculation of shear stress

$$\tau = \frac{V * Q}{I * t} \qquad \bar{y} = \frac{2 * r}{\pi} \qquad r = \frac{r_1 + r_2}{2}$$

$V = 372\ N$

$t = 0.015\ m$

$$I = \frac{\pi}{4}(r_2^4 - r_1^4) = 1.010 * 10^{-8}$$

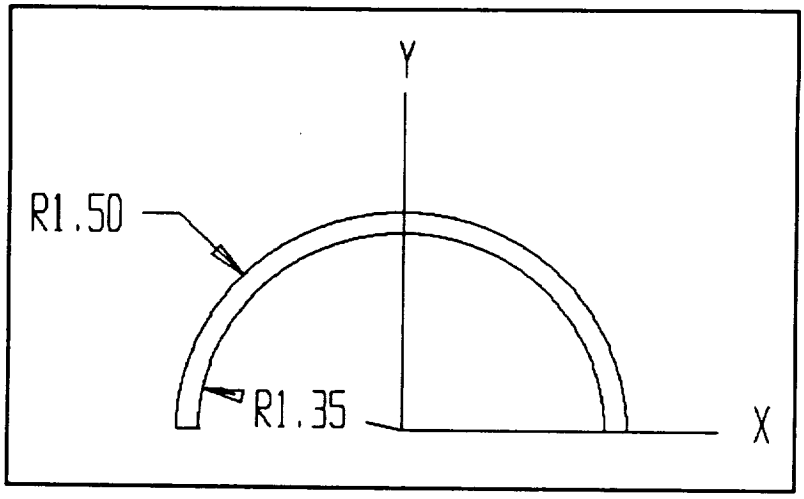

FIGURE A-2

$$Q = A * \bar{y}$$

$$Q = \frac{1.343 * 10^{-4}}{2} * \frac{0.0140 + 0.0125}{\pi} = 5.664 * 10^{-7}$$

$$\tau = \frac{1.5 * 372 * 5.664 * 10^{-7}}{1.010 * 10^{-8} * 0.015} = 1.916 * 10^{6}\ N/m^2$$

$$\tau = 1.916 * 10^{6}\ N/m^2 \times \frac{1\ psi}{6895\ N/m^2} = 277.9\ psi$$

$\tau = 0.2779$ ksi < 12.6 ksi (shear strength of graphite/epoxy)

REFERENCES

(1) Arif, Hugh, Aydelott, John C., and Chato, David J., "Evaluation of Supercritical Cryogen Storage and Transfer Systems for Future NASA Missions," Paper N90-10912, January 1990.

(2) Barnett, Allen, and Rhoads, Sandra, "Modelling and Design of High Performance Indium Phosphide Solar Cells", Paper N89-24712, 1989.

(3) Bate, R.R., Mueller, D.D., and White, J.E., Fundamentals of Astrodynamics, Dover Publications, Inc., New York, 1971.

(4) Beattie, J.R., Matossian, J.N., and Poeschel, R.L., and Rogers, W.P., and Martinelli, R., "Xenon Ion Propulsion Subsystem", AIAA Paper No. 85-2012, Hughes Research Labs, Malibu, CA./Hughes Aircraft Company, El Segundo, CA./EDAC Inc., Torrance, CA., 1985.

(5) Bechtel, Robert T., and Rawlin, Vincent K., "Performance Documentation of the Engineering Model 30-cm Diameter Thruster", AIAA Paper No. 76-1033, NASA Lewis Research Center, Cleveland, OH., 1976.

(6) Bechtel, R.T., Trump, G.E., and James, E.J., "Results of the Mission Profile Life Test," AIAA Paper No. 82-1905, NASA Marshall Space Flight Center, AL./Xerox/EOS, Pasadena CA.

(7) Biron, J., "An Aluminum Collapsible Bladder Tank for Space Systems," AIAA Paper 90-2058, 26th Joint Propulsion Conference, Orlando, FL, July 1990.

(8) Braun, Robert D., and Blersch, Donald J., "Propulsive Options for a Manned Mars Transportation System", AIAA Paper No. 89-2950, Vigyan Research Associates, Hampton, VA./ANSER, Arlington, VA., 1989.

(9) Brophy, J.R., and Aston, G., "A Detailed Model of Ion Propulsion Systems", AIAA Paper No. 89-2268, Electric Propulsion Laboratory, Inc., Lancaster, CA., 1989.

(10) Byers, David C., Terdan, Fred F., and Myers, Ira T., "Primary Electric Propulsion for Future Space Missions", NASA TM-79141, NASA Lewis Research Center, Cleveland, OH., 1979.

(11) Byers, D. C. and Rawlin, V. K., "Electron Bombardment Propulsion System Characteristics For Large Space Systems," 12th Annual International Electric Propulsion Conference Technical Paper, Key Biscayne, FL, November 1976.

(12) Byers, David C., "Upper Stages Utilizing Electric Propulsion", NASA TM-81412, NASA Lewis Research Center, Cleveland, OH., 1980.

(13) Byers, David C., "Characteristics of Primary Electric Propulsion Systems", NASA TM-79255, NASA Lewis Research Center, Cleveland, OH., 1979.

(14) Carney, Michael J., "Liquid-Vapor Interface Locations in a Spheroidal Container," NASA TM 87147, April 1986.

(15) Collett, C.R., and Bechtel, R.T., "An Endurance Test of a 900 Series 30-cm Engineering Model Ion Thruster", AIAA Paper No. 76-1020, Hughes Research Labs, Malibu, CA./NASA Lewis Research Center, Cleveland, OH., 1976.

(16) Collett, C.R., and Poeschel, R.L., "A 10,000 Hour Endurance Test of a 700 Series 30-cm Engineering Model Thruster", AIAA Paper No. 76-1019, Hughes Research Labs, Malibu, CA., 1976.

(17) CRC Handbook of Chemistry and Physics, CRC Press, Inc, 1984, 65th Edition.

(18) Fearn, D.G., and Wallace N.C., "Advanced Propulsion Systems for Space Station Applications", Space Department, Royal Aircraft Establishment, Farnborough, Hampshire, England. In Space Technology, Vol.8, No.4, 1988.

(19) Freas, Charles E., "Solar Electric Propulsion as an Option for a Manned Mars Vehicle", NASA Vehicle Analysis Branch, Space Systems Division, Langley Research Center, Hampton, VA.

(20) Friedly, Verlin Joe. "Hollow Cathode Operation at High Discharge Currents", NASA CR-185238, NASA, Washington D.C., 1990.

(21) Gagliardi, Robert M. Satellite Communications. Von Nostrand Reinhold : New York, 1991.

(22) Galecki, Diane L., and Patterson, Michael J., "Nuclear Powered Mars Cargo Transport Mission Utilizing Advanced Ion Propulsion", AIAA Paper No. 87-1903, Sverdrup Technology, Inc., Lewis Research Center Group, Brook Park, OH./Lewis Research Center, Cleveland, OH., 1987.

(23) Gavaghan, Helen. "Communication Breakdown - Mars Mission," New Scientist. v. 120, pg. 18, Oct 8, 1988.

(24) Gilland, J.H., Myers, R.M., and Patterson, M.J., "Multimegawatt Electric Propulsion System Design Considerations", AIAA Paper No. 90-2552, Sverdrup Technology, Inc./NASA Lewis Research Center, Cleveland, OH., 1990.

(25) Hickman, J.M., Curtis, H.B., Kenny, B.H., and Sefcik, R.J., "Sytems Analysis of Mars Solar Electric Propulsion Vehicles", AIAA Paper No. 90-3824, NASA Lewis Research Center, Cleveland, OH., 1990.

(26) Igenbergs, E., and Kirschner, M., "A Modular Propulsion System for the Interorbital Vehicle", Lehrstuhl fur Raumfahrttechnik, Technische Universitat Munchen, Postfahc 202420, 8000 Munchen, F.R.G., 1986.

(27) Kaufman, H.R., "Performance of Large Inert Gas Thrusters," AIAA Paper 81-0720, 15th International Electric Propulsion Conference, Las Vegas, NV, April 1981.

(28) Kaufman, H.R. and Robinson, R.S., "Large Inert Gas Thrusters," AIAA Paper 81-1540, 17th Joint Propulsion Conference, Colorado Springs, CO, July 1981.

(29) Labus, T.L., and Cochran, T.H., "Space Station Electrical Power Systems," Space Technology. vol. 8, no. 4, pp. 319-328, 1988.

(30) Laurini, D., von Rohden, H., Bartoli, C., and Berry, W., "Field Mission Electric Propulsion (FEEP): Steady and Pulsed Modes of Operation", ESA/ESTEC Technical Directorate Noordwijk, The Netherlands.

(31) Lillington, D.R., et al., "Gallium Arsenide Welded Panel Technology for Advanced Spaceflight Applications," Spectrolab, Inc./Spire Corporation, Paper No. N89-24731, 1989.

(32) Louis A. Teichman and Bland A. Stein, "NASA/SDIO Space Environmental Effects on Materials Workshop," NASA Conference Publication 3035, Hampton, VA, July 1988.

(33) Mackie, J.B. The Elements of Astronomy for Surveyors. Charles Griffin and Company : London, 1978.

(34) Mantenieks, M.A., Sovey, J.S., Myers, R.M., Haag, T.W., Raitano, P., and Parkes, J.E., "Performance of a 100kW Class Applied Field MPd Thruster", NASA TM-102312, NASA Lewis Research Center, Cleveland OH./Sverdrup Technology, Inc., NASA Lewis Research Center Group, Cleveland, OH., 1989.

(35) Martin, A.R., and Cresdee, M.T., "The Use of Electric Propulsion on Low Earth Orbit Spacecraft", UKAEA Culham Laboratory, Abingdon, Oxon OX14 3DB, England. In Journal of the British Interplanetary Society, Vol.41, pp.175-182, 1988.

(36) Myers, R.M., and; Mantenieks, M., and Sovey, J., "Geometric Effects in Applied-Field MPD Thrusters", AIAA Paper No. 90-2669, Sverdrup Technology, Inc., Lewis Research Center Group, Brook Park, OH./Lewis Research Center, Cleveland, OH., 1990.

(37) Piszczor, Michael F., and Mark J. O'Neill, "Domed Fresnel Lens Concentrator Technology for Space Application," NASA Lewis Research Center/Entech, Inc., Paper No. N89-24732, 1989.

(38) Piszczor, Michael F., Swartz, Clifford K., and O'Neill Mark J., "Component & Prototype Panel Testing of the Mini-Dome Fresnel Lens Photovoltaic Concentrator Array," NASA Lewis Research Center, Cleveland, OH./ENTECH, Inc. DFW Airport, TX., 1990.

(39) Ponchak, Denise S. "Technology Assessment of Alternative Communications Systems For The Space Exploration Iniative," AIAA Paper No. 90-3681, NASA Lewis Research Center, Cleveland, Ohio, 1990.

(40) Rhoads, Sandra L., and Barnett, Allen M. "Modelling and Design of High Performance Indium Phosphide Solar Cells," AstroPower Division/ Astrosystems, Inc./University of Delaware, 1989.

(41) Roy, A.E. Orbital Motion. Adam Hilger Ltd. : Surrey, England, 1978.

(42) Schonberg, W., "Spacecraft Wall Design for Increased Protection Against penetration by Space Debris Impacts," AIAA Paper No. 90-3663, University of Alabama, Huntsville, AL. 1990.

(43) Sercel, J., and Krauthamer, S., "Multimegawatt Nuclear Electric Propulsion; First Order System Design and Performance Evaluation", AIAA Paper No. 86-1202, Jet Propulsion Laboratory, Pasadena, CA., 1986.

(44) Sovey, J.S., "Improved Ion Containment Using a Ring-Cusp Ion Thruster", Journal of Spacecraft and Rockets, Vol. 21, No. 5, NASA Lewis Research Center, Cleveland, Ohio, 1984.

(45) Sovey, J. S., "Characteristics of a 30-cm Diameter Argon Ion Source", AIAA Paper No. 76-1017, NASA Lewis Research Center, Cleveland, OH., 1976.

(46) Sponable, Jess M., and Penn, Jay P., "Electric Propulsion for Orbit Transfer: A Case Study", AIAA Paper No. 87-0985, U.S. Air Force, Wright-Patterson Air Force Base, OH./The Aerospace Corporation, El Segundo CA., 1987.

(47) Stahlman, William. Solar and Planetary Longitudes. University of Wisconsin Press : Madison, 1963.

(48) Stutzman, Warren L. Antenna Theory and Design. John Wiley & Sons, Inc. : New York, 1981.

(49) Taylor, Allan H., Cerro, Jeffery A. and Jackson, L. Robert, "An Analytical Study Of Reusable Flight-Weight Cryogenic Propellant Tank Designs," AIAA Paper 84-0865CP, May 1984.

(50) Tenney, Darrel R., "Structural Materials for Space Applications," Langley Research Center, Paper No. N89-23530, 1989.

(51) Vickers, B., Babel H. and Parechanian H., "Materials and Design Selection for Minimum Weight Pressure Vessels," AIAA Paper 90-2349, 26th Joint Propulsion Conference, Orlando, FL, July 1990.

(52) Wertz, James R., Spacecraft Attitude Determination and Control, Reidel, Boston, 1978.

(53) Wibur, Paul J., "Advanced Electric Propulsion Research - 1989", NASA CR-185237, NASA, Washington, D.C., 1990.

(54) Baggs, L. and Engdahl, E., "Advanced Radiator Concepts", Proceedings of the 24th Intersociety Energy Conversion Engineering Conference, Washington, D.C., August 1989.

(55) Jakubowski, Anthony K., "Notes", Aerospace Engineering Department, Virginia Polytechnic Institute, Blacksburg, VA, Spring 1991.